AMERICAN UNIVERSITY OF BEIRUT

A CALPUFF-BASED DISCOURSE ON AIR QUALITY MANAGEMENT IN CHEKKA

by

KHALED MOHAMMAD GHANNAM

A project
submitted in partial fulfillment of the requirements
for the degree of Master of Science in Environmental Sciences
to the Interfaculty Graduate Environmental Sciences Program
Environmental Technology
of the Faculty of Engineering and Architecture
at the American University of Beirut

Beirut, Lebanon
October 2011

AMERICANUNIVERSITY OF BEIRUT

A CALPUFF-BASED DISCOURSE ON AIR QUALITY MANAGEMENT IN CHEKKA

by

KHALED MOHAMMAD GHANNAM

Approved by:

Dr. Mutasem El-Fadel, Professor Civil and Environmental Engineering	Advisor
Dr. Farid Chaaban, Professor Electrical and Computer Engineering	Member of Committee
Dr. Mahmoud Hindi, Assistant Professor Mechanical Engineering	Member of Committee

Date of project defense: November 1, 2011

AMERICANUNIVERSITY OF BEIRUT

PROJECT RELEASE FORM

I, Khaled Mohammad Ghannam

☐ authorize the American University of Beirut to supply copies of my project to libraries or individuals upon request.

☐ do not authorize the American University of Beirut to supply copies of my project to libraries or individuals for a period of two years starting with the date of the thesis defense.

_____

Signature

_____

Date

ACKNOWLEDGEMENTS

I would like to thank Prof. Mutasem El-Fadel for his continuous guidance towards the completion of this work. I am also grateful to Lakes Environmental Software for their technical support on different aspects of CALPUFF model and for providing access to valuable data. Family and friends are always appreciated for their love and support.

AN ABSTRACT OF THE PROJECT OF

Khaled Mohammad Ghannam for Master of Science
Major: Environmental Technology

Title: A CALPUFF-based discourse on Air Quality Management in Chekka

Ambient air pollution in the vicinity of industrial complexes is a multi-dimensional problem with consequences on the environment, public health and community welfare. Air quality modeling is relied upon for integrated assessments in such contexts, but is often associated with a high degree of uncertainty, particularly when emission magnitudes are unknown and a multitude of sources contributes to ambient air pollution.

In this context, the current study coupled the non-steady state MM5/CALMET/CALPUFF dispersion modeling system with year-round field measurements for a regulatory compliance-based assessment of air quality in the coastal area of Chekka, North Lebanon. In addition to the industrial complex, Highway emissions and quarrying sites were identified as significant emission contributors.

An emission inventory was first developed for emissions of CO, NO_x, SO_2 and PM_{10} from various sources using EPA-AP42 and EEA (Tier 1 and 2) emission factor guidelines, and assessed for their representativeness of the study area using multiple statistical indicators. CALPUFF validation and performance evaluation emphasized its capabilities in regulatory contexts, along with statistical analysis of predicted and observed concentrations, which revealed a good ability of the model in reproducing field measurements at several locations. Apportionment analysis reflected a significant contribution of Highway emissions to CO and NO_2 levels in the study area, with point sources impacting more distant locations. Ambient concentrations of the criteria pollutants in the study area exceeded the USEPA-NAAQS standards during the whole year, except for CO. CALPUFF predictions exhibited negligible sensitivity to coastal fumigation and chemical transformations within the modeling domain. Also, a comparative assessment of CALPUFF with ADMS4 revealed comparable performance of the models in the study area. Last but not least, Compliance of point sources with the ELV improved the air quality in the study area significantly.

Keywords: Dispersion modeling, CALPUFF, Emission factors, Source apportionment

CONTENTS

TABLES

Tables Page

ILLUSTRATIONS

Figure Page

CHAPTER 1

INTRODUCTION

The economic trade-offs between industrial growth and environmental damage continue to be controversial in the contexts of cost-benefit analysis and scientific evidence (Krishna et al. 2005). While developments in the scope, size and density of industrial installations may lead to economic growth in certain aspects, they are associated with direct adverse impacts on public health, as well as environmental externalities (WHO 2006). In particular, ambient air pollution in the vicinity of industrial complexes has become of increasing concern, especially in urban areas where rapid industrial development coupled with emissions from the transport sector are recognized as major sources (Banerjee 2010). Furthermore, urban environments are of particular vulnerability to air quality deterioration due to the large population density residing in such areas and thus high energy consumption, which render air pollution more tangible. On the other hand, the scientific evidence and reliability of air quality studies in such cases is often affected by the absence and/or uncertainty in emission inventories, which list the potentially polluting sources, along with their corresponding emission magnitudes. Emission inventories constitute the cornerstone for effective management plans, and in conjunction with air quality modeling, serve as basic tools for planning of control strategies and mitigation measures to achieve ambient air quality goals (Bhanarkar et al. 2005).

In Lebanon, the bulk of the cement manufacturing industry is centered in the town of Chekka, a coastal area between Beirut and Tripoli. The area comprises multiple facilities with various industrial activities (cement manufacturing, asbestos pipes manufacturing, fertilizers, etc.) and their associated quarrying sites as sources of limestone (Ayash 2002). Aggravated air quality in and around Chekka has been the subject of debate among the public, governmental and international institutions, NGOs and the scientific community (World Bank 1998; Kobrossi et al. 2002; El-Fadel et al. 2009). Field measurements conducted during the year 2003 have shown NO_2, SO_2 and PM_{10} were frequently encountered at elevated concentrations at various locations in the region (Karam and Tabbara 2004). The industrial complex, with unknown emission rates, has been perceived as a major contributor to these concentrations. Recently, El-Fadel et al. (2009) and El-Fadel and Abi-Esber (2011) used the ISCST3 and ADMS4 dispersion models, respectively, in an attempt to estimate the emission rates of various sources, along with a compliance-based assessment of air quality in the area. The current work, and upon a comprehensive review of pertinent literature, coupled the non-steady state CALPUFF dispersion modeling system with field measurements for the year 2003, to define a basis for developing an Air Quality Management Plan (AQMP) around the Chekka industrial complex. While building on previous studies (El-Fadel et al. 2009; El-Fadel and Abi-Esber 2011), this study offers advanced technical treatment of various components of a potential integrated air quality assessment. In particular, an extensive set of dispersion modeling exercises was conducted to assist in identifying important trends and features in the study area. Such simulation sets are intended to assess both the performance of CALPUFF under different scenarios (meteorological and geographic conditions), and the sensitivity of its output to various

initial assumptions. Furthermore, such exercises reflect on the degree of uncertainty in the outcome, and thus allow for drawing reasonable conclusions. For this purpose, the present study comprised the following tasks:

- Estimation of emission rates[a] of various source groups contributing to air pollution in the study area
- Apportionment analysis of source categories contributing to air pollution under different spatial and temporal scales
- Uncertainty and sensitivity analysis under various assumptions
- Comparison of the performance of the two dispersion models (CALPUFF and ADMS4) under the same setting, and
- Proposing mitigation measures for major contributing sources with corresponding impact assessment

This study is presented in an orderly manner where its sub-sections are tailored towards specific objectives, but ultimately synergizing to provide room for drawing reasonable conclusions and sound judgments, always considering limitations and uncertainties. In particular, Chapter 2 presents a literature review of recent research relevant to air quality modeling and management, highlighting various approaches and trends, and attempting to identify future needs in order to bridge gaps among different approaches. Chapter 3 examines the characteristics of the study area, namely the industrial activities and topographic features, along with the methodological framework and modeling scenarios adopted to meet the specified objectives. It also presents the model

[a]A most representative emission rate was assigned for each pollutant out of a set of five derived emission rates

selection and justification process in relation to study area features, and CALPUFF input data enquiry (emission rates and meteorological data). Results and discussion are presented in Chapter 4, starting with a close examination of trends in field measurements, and estimation of representative emission rates. Source apportionment is then addressed and discussed, followed by sensitivity analysis and the inter-model comparative assessment. Though mostly technical involving "research grade" components of atmospheric dispersion modeling, the study frequently analyzes results from a regulatory compliance perspective.

CHAPTER 2

LITERATURE REVIEW

Effective Air Quality Management (AQM) often involves interdisciplinary approaches encompassing scientific, legislative and policy measures. Such integrated approaches are necessitated by the multi-dimensional impacts of air pollution on public health, the physical environment, and community welfare (Longhurst et al. 2000; Cheung et al. 2005; WHO 2006). Scientific assessments of air quality management studies often constitute the fundamental basis for regulatory decision-making and policy implementation thereafter (USEPA 1999), with other factors equally playing key roles in the process (economic, social, etc.). In this context, emissions from industrial complexes in urban and semi-urban areas continue to be under scientific scrutiny, given their association with aggravated air quality in these areas (Krishna et al. 2005; El-Fadel et al. 2009). While such science-based appraisals of air quality are intended to aid decision-makers in defining appropriate measures for emission reduction, and thus compliance assurance, their reliability can often be questionable (Colvile et al. 2002). This is mainly due to uncertainties and data gaps associated with almost every step of developing the scientific assessment, which if not properly considered and managed, render the decision-making and analysis processes quite elusive.

Emissions from industrial facilities vary in magnitude (depending on facility size, production rate, etc.) and pollutant type (depending on fuel characteristics, manufacturing processes, etc.), but frequently comprise the criteria pollutants (CO, SO_2, NO_2, PM_{10}) and

their precursors. Quantifying the magnitude of these emissions from a facility's stack under operation, for instance, is necessary to ensure its compliance with the Emission Limit Values (ELV), which are established by international and national institutions to protect public health and the environment (USEPA 1996). As such, emission inventories became an essential component of the AQM process, as they quantitatively measure and monitor emissions from different sources (point, area or line sources), and thus reflect on the need to take actions for emission reduction (Denby et al. 2009). The quality of such data can affect the credibility of an integrated assessment of air quality in a given region, as it is required as input for atmospheric dispersion models, which are in turn sensitive to these data and might thus yield unreliable outcomes.

In practical settings, where a multitude of sources contribute to emissions and thus concentrations of pollutants at various receptors, the regulatory analysis becomes more complex, especially if the source strengths are not known. Receptor modeling can be relied upon in such cases, which involves inverse dispersion modeling, source profiling, Principal Component Analysis (PCA) and Chemical Mass Balance (CMB) approaches. These modeling techniques aim at assigning relative contributions of sources to pollutant concentration at a particular receptor (Watson and Chow 2004; Hopke 1991). However, such approaches are resource-demanding, spatially limited to the studied receptor (Laupsa et al. 2009), and still exhibit a high degree of uncertainty (Hueglin et al. 2000). On the other hand, atmospheric dispersion models are also used in this context (source apportionment and regulatory analysis). These models are intended to assess the ambient air quality at a desired receptor or region due to different sources, as temporal and spatial

monitoring of pollutants is not always feasible due to high cost and experimental difficulties. Dispersion models offer an alternative in regulatory contexts to predict the fate and transport of pollutants and most importantly, forecast and assess future management scenarios (Prabha and Singh, 2006).

Source apportionment and attribution analysis using atmospheric dispersion models has been examined to assess and manage industrial emissions (Denby et al. 2009; Fushimi et al. 2005). This is particularly important from a risk assessment and environmental justice standpoint, as to what sources need to be targeted for abatement measures, while simultaneously predicting how would air quality respond to implementing such measures (John and Karnae 2011). However, applications of such techniques require good emission inventories of potentially contributing sources and validation of the dispersion model. While sources could be cautiously characterized based on internationally reported data of similar industries, the latter is a crucial step prior to any analysis. In essence, model validation addresses the suitability of using a particular atmospheric dispersion model under certain conditions, based on its ability to successfully predict, to a reasonable degree, measured concentrations at different locations and time periods (Woodfield et al. 2003). Given that models are mathematical representations of natural processes, their outcomes are fairly often associated with uncertainties. Among many others, Chang and Hanna (2004) proposed a set of statistical parameters and data plots that could evaluate the performance of atmospheric dispersion models, and thus the applicability of a model for an air quality study. It is stressed however, that the choice of such parameters depends primarily on the ultimate objective of the study. For instance, regulatory applications of

dispersion modeling require the model to predict the higher end of a measured concentration distribution, with less emphasis on its ability to accurately capture fluctuations in the concentration field. These uncertainties in dispersion modeling could be attributed to a multitude of sources including, but not limited to, random turbulence in the atmosphere, errors and uncertainties in model physics, and input data errors (Fox 1984; Anthes et al. 1989; Hanna et al. 1991; and Beck et al. 1997). Equally important, are considerations of unrepresentative instrument siting and measurement errors. In the interest of conciseness, Table 1 below summarizes recent studies that employed atmospheric dispersion modeling to source apportionment analysis in regulatory contexts, along with others of pertinence to this study, for the purpose of comparative assessment whenever applicable.

Table 1. Selected list of recent studies consulted in this study

Reference	Objective and Methodology	Model used
Levy et al. (2002)	Studied the health impacts of nine major power plants in Illinois-United States. In particular, the incremental changes in $PM_{2.5}$ concentrations and thus the impacts were analyzed against the sensitivity of the CALPUFF model to different assumptions (chemical transformations and wet/dry deposition). The impacts were assessed to be moderately insensitive to those assumptions	CALPUFF[a]
Husain et al. (2003)	Compared the performance of ISC3, HYSPLIT and CALPUFF in a coastal area. CALPUFF predictions of SO_2 concentrations matched observations better	CALPUFF, ISC3, HYSPLIT[b]
Fushimi et al. (2005)	Developed a source apportionment methodology based on atmospheric dispersion modeling and Multiple Linear regression (MLR). Started with reported emissions rates for different sources of Benzene in an industrial area in Japan. Model predictions did not meet observations, and emission rate was assumed incorrect. Based on the contribution of each source assessed by the model, they developed regression coefficients for each source and rescaled their emission factors.	ISCST3[c]: regulatory (EPA-approved) Gaussian dispersion model (Local scale)

Barna et al. (2006)	Studied the contribution of different regions (sources) to the sulfate-induced Big Bend National Park (BBNP) haze, as part of the Big Bend Regional Aerosol and Visibility Observational Study (BRAVO) through a dispersion modeling source apportionment scheme. Designed a suite of emissions-sensitivity simulations to test the model linearity prior to source apportionment. The model responded linearly to changes in emission rate. This was used to reflect on what source contributions (emissions) were over/underestimated	REMSAD[d]: is an Eulerian-grid air quality model designed to simulate the formation and transport of aerosols and their precursors on a regional scale
Denby et al. (2009)	Compared source attribution analysis resulting from receptor modeling (Positive Matrix Factorisation), dispersion modeling and MLR to optimize source emission rates. The study addressed $PM_{2.5}$ concentration at a traffic monitoring station in Oslo. Source strengths used in the dispersion model were refined and simulations were re-run for predictions to meet the observations	Air-Quis: Norwegian Institute for air research
El-Fadel et al. (2009)	Used ISCST3 for a regulatory compliance study. They derived a set of emission factors for a multi-stack industrial complex in Chekka, North Lebanon. Emission factors of CO, NO_x, SO_2 and PM_{10} were based on EPA-AP42 and EEA guidelines, and spanned values representing minimum, maximum and worst cases. These were coupled with actual and worst meteorological conditions to conduct a conservative assessment of air quality in the area. ISCST3 was validated against CO field measurements and exhibited good performance. Mitigation measures and control strategies were proposed and assessed, showing significant improvement in spatial distribution of affected areas.	ISCST3
Lau et al. (2010)	Source apportionment of major SO_2 sources in the Hong-Kong Special Administrative Region. Sources included power plants, marine vessels, and vehicles in a complex terrain. Source contributions were assessed at different locations and during different seasons to address major contributors for an air quality management plan	CALPUFF: an advanced non-steady state Gaussian-Lagrangian puff model. USEPA-approved for mesoscale transport in regulatory contexts.
MacIntosh et al. (2010)	Used CALPUFF in a near-field complex terrain setting to predict deposition fluxes of various metals emitted from industries, in an exposure assessment study. CALPUFF was able to reflect spatial variations of metal concentrations measured in attic dust samples	CALPUFF
Abdul-Wahab and Al-Damkhi (2011)	Used CALPUFF in a coastal area with complex terrain to simulate the dispersion of SO_2 emissions from a refinery in Oman. Results were compared with those of the same study done with ISCST3. CALPUFF predictions matched observations better	CALPUFF, ISCST3

EL-Fadel and Abi-Esber (2011)	Used ADMS4 coupled with field measurements in the vicinity of an industrial complex in Chekka, North Lebanon. They defined a set of emission factors for the industrial facilities, vehicular emissions, and open pit(area) sources using EPA-AP42 and EEA (Tier1&2) guidelines, which was used as input for ADMS4 in an attempt to estimate representative emission rates through statistical analysis. The conservative estimates of emission rates were assessed as representative.	ADMS4[e]

[a/]California Puff dispersion model
[b/]Hybrid Single Particle Lagrangian Integrated Trajectory Model
[c/]Industrial Source Complex Short Term model
[d/]The Regional Modeling System for Aerosols and Deposition
[e/]The Atmospheric Dispersion Modeling System Version

The studies cited in the above discussion and in Table 1 reveal a variable degree of complexity and uncertainty in the adopted methodological approaches. While some studies coupled inverse modeling and backward Lagrangian systems (bLS) with forward modeling (dispersion modeling) in a comparative manner to arrive at adequate estimates of uncertain emission rates, others relied on short-term measurements and monitoring for the same purpose. Few studies, if any, attempted to derive a set of emission rates that span a range of values, primarily due to the associated complexity. Such a range allows for an assessment of worst and best-case emissions scenarios, particularly that the emissions pattern from industrial activities is likely to change temporally. In comparison, this study relied on extensive statistical analysis to evaluate the representativeness of each derived emission rate under several spatial and temporal scales, which alleviates the complexity and resource-demanding approaches mentioned above. Furthermore, to our knowledge, the linearity and emissions sensitivity of CALPUFF have not been addressed in the context of source apportionment studies, most of which assumed that CALPUFF is summing the contributions of various sources at a downwind receptor. While our study shows that this

assumption is valid, it emphasizes this fact and may serve as a reference for future source apportionment assessments to be conducted in a more economic manner.

CHAPTER 3

MATERIALS AND METHODS

3.1 Study Area Characteristics

The study area lies along the Eastern Mediterranean(Lat. $34^0$27'N and Long. $35^0$34'E), at around 55 km to the north of the capital of Lebanon, Beirut, and 16 km to the south of the second largest city, Tripoli (Figure 1). The bulk of the industries is clustered in the coastal town of Chekka (LO2 in Figure 1). Other potential sources contributing to air pollution in the region include vehicular emissions (Highway) and quarrying sites. While other sources might be potentially contributing, they were deemed less significant. Figure 1 also shows five monitoring sites (LO1-LO5) corresponding to five nearby towns, namely Enfeh, Chekka, Fih, Kfarhazir and Kefraya respectively. Ambient concentrations of CO, SO_2, NO_2 and PM_{10} were measured on a rotational basis for one to two weeks at each of these locations during the year 2003 (Karam and Tabbara 2004). Topographically, the area qualifies as a mixture of urban, semi-urban to the west, and rural to the east, with a relatively complex terrain setting. Figure 2 shows the transitions in the terrain elevations above the Mean Sea Level (MSL), along with the locations of the villages/towns where the monitoring stations were installed.

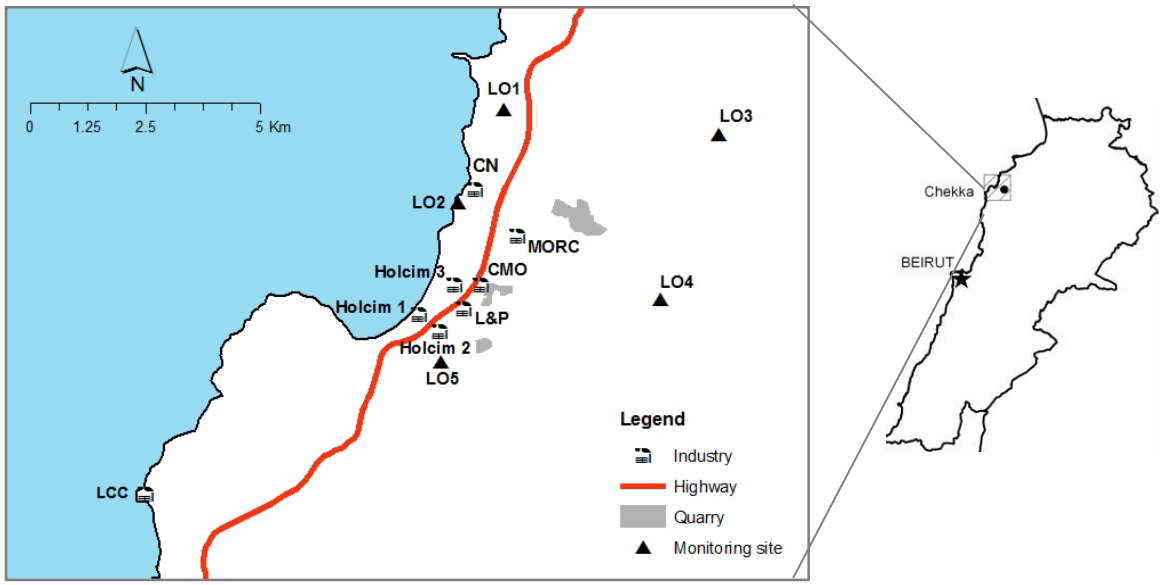

Figure 1. Illustrative map of the study area with sources and discrete receptors

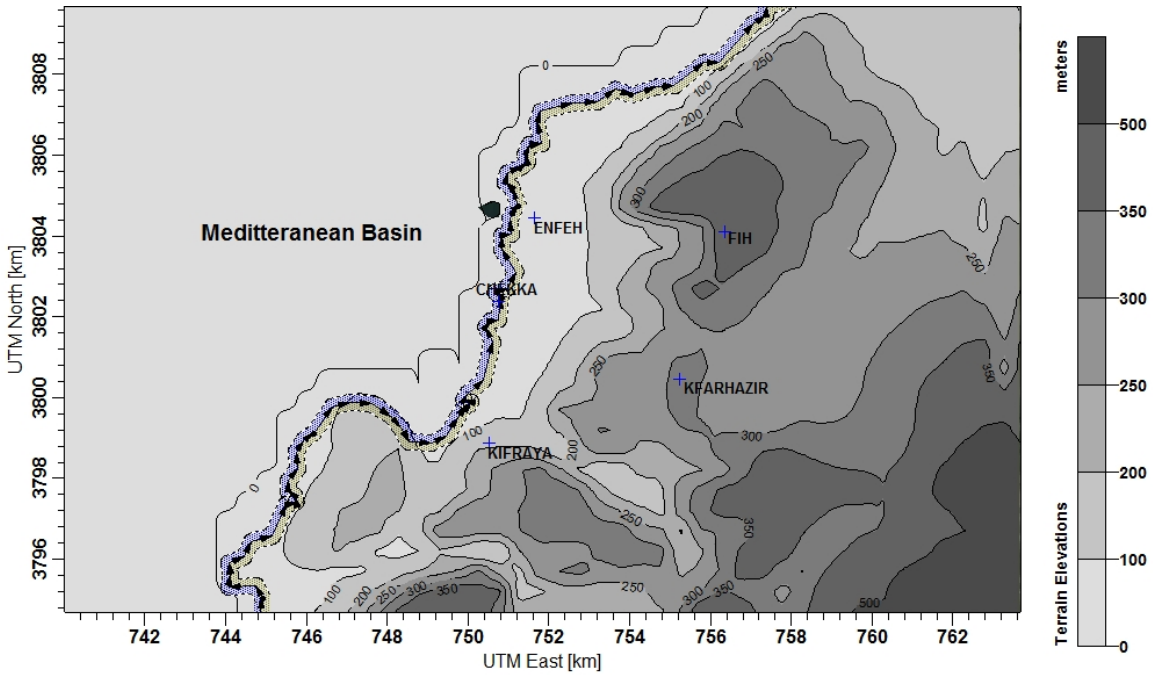

Figure 2. Contour lines of terrain elevations within the study area

While Chekka and Enfeh receptors are on a flat terrain close to the coastline, the others are on a relatively elevated and complex terrain. Namely, Fih and Kfarhazir lie on hilly areas at around 350-400m above MSL, while Kifraya is at about 200m above MSL. Such terrain complexity may contribute to temporal and spatial variability in meteorological conditions, such as slope flows, reversals and blocking effects, which in turn enhance the atmospheric turbulence capacity. Climatologically, the study area is of the sub-tropical, Mediterranean type with warm and dry summer and fall, and moderately cold, windy and wet winter. The prevailing wind direction is North-East with a frequency of more than 30%, and relatively low wind speed of less than 5m/s for 60% of the year.

The characteristics of the industrial plants considered as emitting sources in the study area are summarized in Table 2, namely the industrial activity, production rate, energy and process fuel, and the control measures reported to be in place. Ayash (2002) presents a detailed description of the various activities within each plant.

Table 2. Characteristics of the main plants in the study area

Industry name	*Production*				*Process fuel*		*Energy fuel*	
	Process	*Product(s)*	*Emission control* [b/]	*Rate (t/d)*	*Type*	*Quantity (t/d)*	*Type*	*Quantity (t/d)*
Holcim (1 &2)	Dry/preheater/ precalciner	Clinker	ESP, BHF, C	5,800	Petcoke	580	Fuel oil	77
		Grey cement		3,190				
Holcim (3)	Dry/preheater	Clinker	ESP, BHF, C	300	Petcoke	39	–	–
		White cement		167	Fuel oil	47		
CimenterieNationale (CN)	Dry/preheater/ precalciner	Clinker	ESP, BHF, C	2,900	Petcoke	480	Fuel oil	140
				2,000	Fuel oil	54		
		Grey cement		1,380				
Seament (CMO)	Dry/preheater	Clinker	ESP, BHF, C	200	Fuel oil	22	Fuel oil	1.7
		Grey cement		52				
Lime & Plaster Co. (L&P)	Rotary kiln/ore/ calciner	Lime	BHF	8.2	Fuel oil	2.7	–	–
		Plaster		1.8				

Mineral Oil Recycling Co. (MORC)	Traditional batch	Base/lube oil		5.6	Gas oil	0.21	–	–
Lebanon Chemicals Co. (LCC)	Double contact/Rhone-Poulenc	Sulphuric acid	WS	650	Fuel oil	33	–	–
		Phosphoric acid		200				
		TSP fertilizer		183				
		SSP fertilizer		83				

[a/] Source: El-Fadel*et al*., 2009
[b/] ESP: electrostatic precipitator; BHF: baghouse filter; C: cyclone; WS: wet scrubber

3.2 Field Monitoring

An environmental monitoring station (EMS) capable of logging measurements of air quality indicators such as CO, NO_2, SO_2, wind speed, wind direction, relative humidity and temperature was installed at Chekka, Enfeh, Fih, Kfar-hazir and Kefraya on a rotating schedule. In addition, PM_{10} readings were recorded using an SKC Split 2 real-time dust monitor. Time-average meteorological and air quality indicators were computed using 30-min or 10-min instantaneous EMS readings and 10-s and 1- to 5-min average PM_{10} readings. The short sampling time for PM_{10} measurements limited the monitoring period to a one-day basis, for 42 discrete days of the base year 2003. The averaging time for all the records was normalized to a one-hour average (to be compared to model's output). The field dataset was also examined for discrepancies that could be attributed to measurement errors. In particular, measurements of nil values were replaced by the instrument's Limit of Quantitation (LOQ) (0.001 ppm at STP), as they were assumed to fall below the instrument's measurement threshold. Moreover, records showing repetitive trends where measurements infrequently meander around a constant value were excluded from the

analysis. Table 3 summarizes the monitoring periods at each site, along with the sampling time intervals. The period covered by the measurements spans over ten months and covers the two dominant meteorological regimes of Lebanon, the warm and dry season which usually spans from May to October, and the wet season which spans from November to April.

Table 3. Summary of field monitoring campaign for CO, NO_2 and SO_2

Location	Monitoring period[a/]	Sampling intervals (minutes)
Enfeh	31 Dec 2002 – 11 Jan 2003	30
Chekka	11 Jan 2003 – 2 Feb 2003	30
Fih	3 Feb 2003 – 19 Feb 2003	30
Kfar-hazir	1 Mar 2003 – 15 Mar 2003	30
Kefraya	15 Mar 2003 – 23 Mar 2003	30
Enfeh	19 Apr 2003 – 13 May 2003	10
Chekka	13 May 2003 – 20 May 2003	10
Fih	15 Jun 2003 – 6 Jul 2003	30
Kefraya	15 Jun 2003 – 5 Jul 2003	30
Kfar-hazir	5 Jul 2003 – 16 Aug 2003	30
Fih	26 Aug 2003 – 6 Sept 2003	30
Chekka	6 Sept 2003 – 23 Sept 2003	30
Enfeh	9 Sept 2003 – 5 Oct 2003	30

[a/] PM_{10} monitoring was conducted at selected days during each period for a total of 42 days

3.3 Statistical Analysis

The performance of the air quality model (CALPUFF) was evaluated using several statistical indicators (Fractional Bias (FB), Geometric Mean Bias (MG), Normalized Mean Square Error (NMSE), and the fraction of predictions within a factor of two of observations (FAC2)) and data plots correlating model predictions with field measurements (Equations 1-4).

$$FB = \frac{(\overline{C_o} - \overline{C_p})}{0.5(\overline{C_o} + \overline{C_p})} \Rightarrow \frac{\overline{C_p}}{\overline{C_o}} = \frac{1 - 0.5FB}{1 + 0.5FB} \quad (1)$$

$$MG = \exp(\overline{\ln C_o} - \overline{\ln C_p}) \quad (2)$$

$$NMSE = \frac{\overline{(C_o - C_p)^2}}{\overline{C_o}\,\overline{C_p}} \quad (3)$$

$$FAC2 = \text{Fraction of data satisfying the expression } 0.5 \leq C_p/C_o \leq 2 \quad (4)$$

C_o and C_p are the observed and predicted concentrations respectively, and the over bar represents the average of a dataset. FB is a linear measure, and reflects on the degree of matching between the predicted and observed mean of the concentration distribution. It is bound between -2 and +2, and a perfect model would result in FB=0 (predicted mean is equal to observed). An FB=0.67 for instance, reflects a factor of two under-prediction of the mean, while negative values depict over-predictions. MG is also linear, and reflects on the degree of bias of the geometric mean rather than the arithmetic mean. A perfect model would result in MG=1, and an MG=0.25 or 4 for example, indicates a factor of 4 over or under-prediction of the mean, respectively. NMSE measures the relative scatter of the distribution. For instance, say the predicted and observed means are equal, an NMSE=1 tells that the root mean square error is equal to the mean. As NMSE becomes much larger than 1, it can be inferred that the distribution is not normal (many low values and a few large values for example). FAC2 is the most robust measure, as it reflects the percentage of predicted concentrations lying within a factor of two of observations.

Quantile-Quantile (Q-Q) and time series plots were also used to provide a visual insight on the model's performance. Q-Q plots rank each of the predicted and observed concentration data separately from lowest to highest, thus the 1st highest predicted concentration would be plotted against the 1st highest observed concentration, which would reveal model biases at low or high concentrations.

3.4 Framework and Definition of Simulations

The methodology proposed to meet the objectives mentioned above is multi-tiered, where different levels of analytical tools are used, ranging between simple data plots and visual inspections to complex statistical and technical analysis. Figure 3 concisely outlines the approach adopted in the study. The 13 monitoring periods (see Table 3) at 5 locations (LO1 to LO5) were coupled with 5 derived emission factors (EEA_{min} to EPA_{max}) to yield a 65 base-case simulations set, which provided sufficient results for statistical analysis of emission rates estimation.

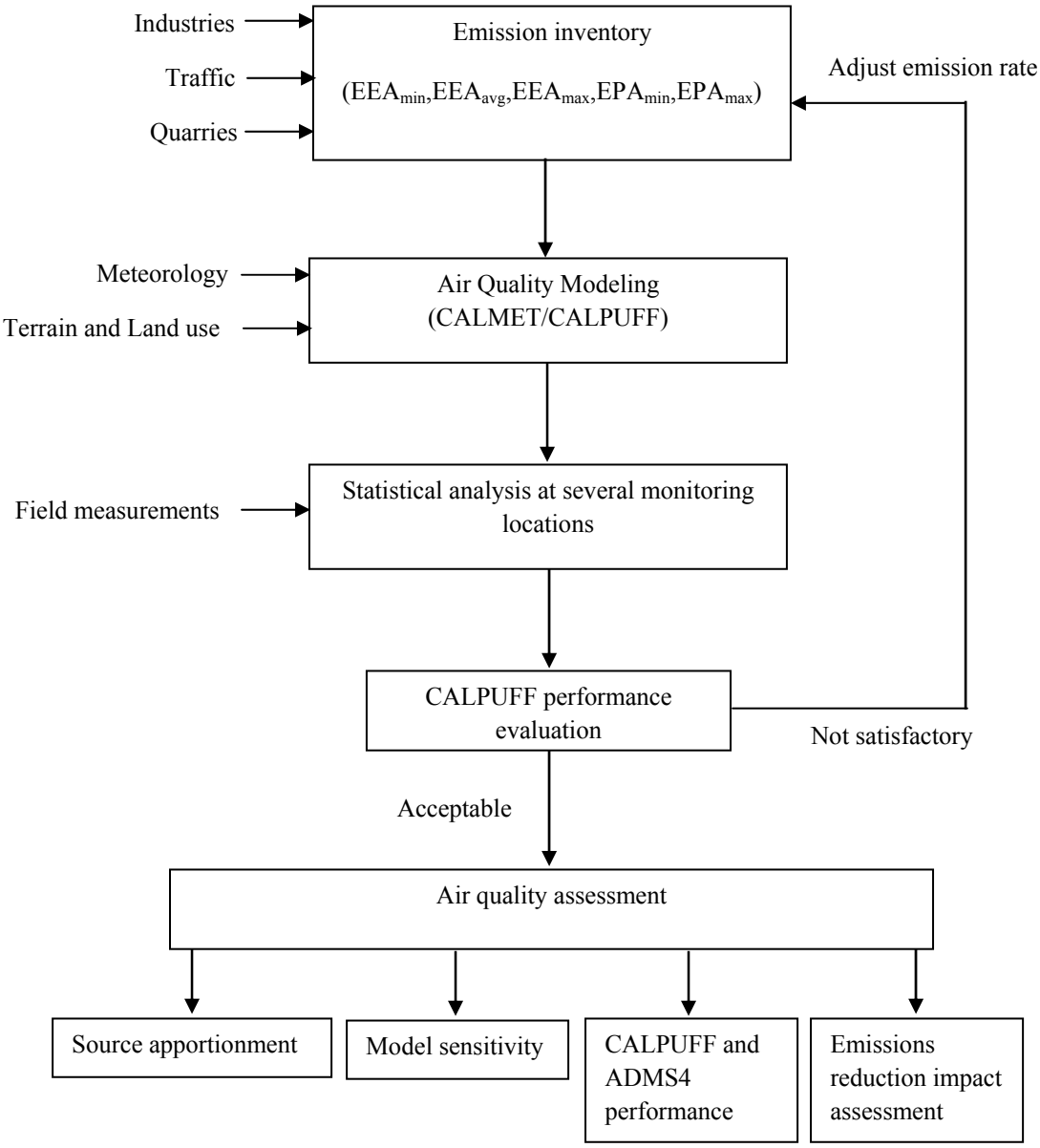

Figure 3. Flowchart of the methodological framework

The concurrent model validation and emission rate estimation proposed in the methodological framework (Figure 3) might be deemed counter-argumentative. While the iterative framework of changing the emission rate assumes that the model will be able to predict observations whenever fed with the representative emission rate, this might not be

always the case. For instance, even if the model was fed with the representative emission rate, it might fail to predict observations at some receptors, or at the same receptor but at different time periods (surrogate measure of meteorological conditions). Equally important, is that model predictions might match observations at a particular receptor when using a certain emission rate, but perform comparably well at another receptor using another rate. This issue was resolved by inspecting prevailing meteorological conditions at the receptor of interest during the run period, and by aggregating the measured and predicted datasets at that receptor for all run periods. Also, it is assumed that the emission rate at which the model reasonably predicts observations most frequently, i.e. at many receptors and run periods, is judged as representative, always with bias towards conservative estimates to reflect on worst-case conditions.

Once an emission rate is assumed for the sources, source apportionment is conducted at different receptors to assess the contribution of each source category and the likelihood of over/underestimations. In the interest of comparative assessment, the sources were broadly categorized as point (Industrial facilities in Table 2), line[2] (Highway), and area sources (quarrying sites). Source apportionment was conducted by designing a set of emissions-sensitivity simulations to test the linear response of the model to gross changes in the emission rate assumed (Barna et al. 2006). With the "base-case simulations" at hand (these are simulations where all sources were included and considered to be emitting at the estimated emission rate), the contribution of a particular source to the pollutant concentration at a certain receptor can be evaluated in two ways:

[2]Highway emissions were simulated as an extended area source with dimensions equal to the length and width of the highway, but referred to as line source to distinguish them from quarrying sites

a) “Emissions-in” approach: this scenario for a simulation sets the emission rate of all sources to zero, except for the source to be assessed. The contribution of this particular source to the receptor will simply be the predicted concentration.
b) “Emissions-out” approach: this scenario is the same as the “base-case”, (all sources emitting), but removes only the emissions from the source to be assessed. The source contribution is thus the difference between the predicted concentration in the “base-case” and the predicted concentration in the “emissions-out” simulation.

This approach is intended to test the linearity of CALPUFF in responding to changes in precursor emissions, and provides an insight on rescaling of emission factors down the line. In essence, for a given source, the model is assumed to be linear if the sum of the concentration predicted in the “emissions-in” and “emissions-out” simulations is equal to that predicted in the “base-case”. However, this might not be valid for reactive pollutants, which are subject to chemical transformations in the atmosphere that are dependent on the ambient concentration of these pollutants. Sensitivity analysis of the model’s output to chemical transformations was thus carried out, and assessed as to what degree it affected the emission rate estimation and other uncertainties in the results. Furthermore, sensitivity of the model’s performance to the Thermal Internal Boundary Layer (TIBL) effect, which leads to coastal fumigation of plumes was considered, especially to reflect on its effect on the behavior of the emitted plumes, and consequently on near-source receptors.

3.5 Model Selection and Description

Atmospheric dispersion models are indispensible tools to assess the impact of emissions from a certain source on air quality. Rather than replicating atmospheric processes accurately, they are intended to mathematically approximate the dispersion of pollutants in the atmosphere taking into consideration meteorological conditions, and thus predict the concentration of a pollutant at a given location. In regulatory contexts of air quality assessments, Gaussian-based models are highly relied upon, as they are simple to use, and exhibit acceptable predictive capabilities (Holmes and Morawska, 2006). Gaussian models are based on a Gaussian (normal) distribution of the plume in the vertical and horizontal directions under steady state conditions (homogeneous wind field). The normal distribution of the plume is modified at greater distances due to the effects of turbulent reflection from the surface of the earth and at the boundary layer when the mixing height is low. The width of the plume is determined by σ_y and σ_z (dispersion coefficients), which are defined either by stability classes (Pasquill 1961; Gifford 1976) or travel time from the source. One limitation of Gaussian-plume models is that they use steady state approximations, allowing the plume to evolve only spatially, and thus do not take into account the time required for the pollutant to travel to the receptor. Additional limitations are related to their inability to treat calm hours (low wind speeds <0.5m/s), and therefore over-predict concentrations at near-source receptors (Benson 1984; Sokhi et al. 1998). In its guidance on air dispersion modeling from industrial installations, the USEPA developed a model selection framework among three regulatory models, AERMOD, ADMS4 and CALPUFF (Figure 4) (USEPA 2008).

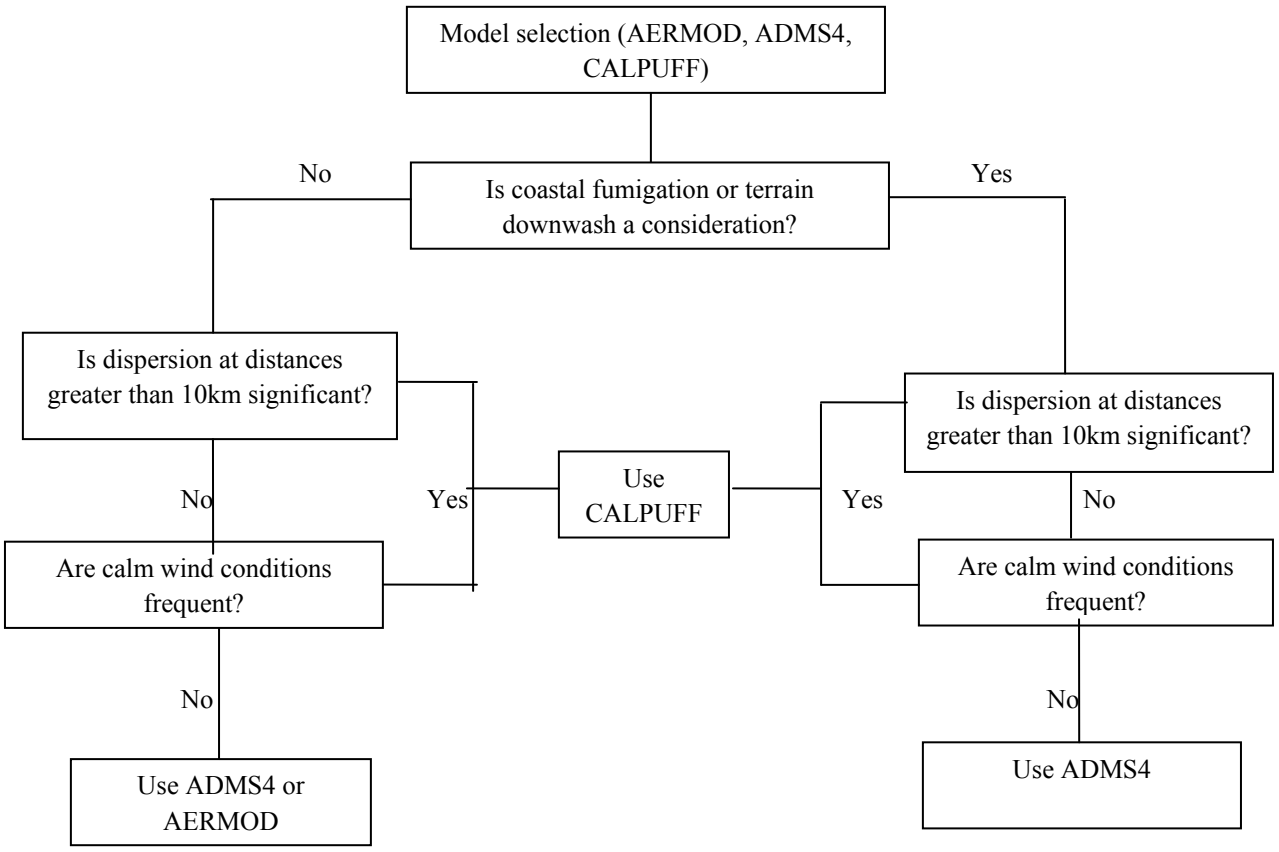

Figure 4. Model selection framework (adapted from USEPA 2008)

The California Puff (CALPUFF) model was used in this project, as it has the ability to account for the spatial variability and non-steady state meteorological conditions within the modeling domain, which are considered to be significant within the study area, given the terrain complexity and land use variability. Equally important, coastal fumigation and regions of stagnation (calm hours), which are also relevant to the modeling domain, are beyond the capabilities of AERMOD and ADMS4. CALPUFF has the USEPA regulatory status for long range transport (between 50and 200km) (USEPA 2005), and on a case-by-case basis in near field applications, particularly in cases where the steady-state assumptions of Gaussian models are questionable.

CALPUFF is a multi-layer, multi-species non-steady-state Gaussian puff dispersion model that simulates the effects of time and space-varying meteorological conditions on pollutant transport, transformation, and removal. As opposed to traditional Gaussian plume models, CALPUFF simulates the continuous plume from a source as a series of discrete "puffs" (packets of pollutants) (Scire 2000), that are transported and dispersed through a 3-D wind and micro-meteorological field, generated by its meteorological processor, CALMET. Each "puff" however, still behaves according to the Gaussian dispersion equation, but the emissions discontinuity allows the released puffs to meander with the time-varying wind field. The contribution of each puff to the concentration at a receptor is calculated by a "snapshot" approach, where the puff is frozen at particular time intervals (sampling times, usually one-hour), sampled, and then allowed to evolve in size and strength. The concentration at a receptor for a time step is then calculated by summing the contribution of all nearby puffs for the basic time step. To this end, Table 4 summarizes some of the important features of the CALPUFF system in comparison to other models.

Table 4. Important characteristics of the CALPUFF modeling system

Features	CALPUFF
Geophysical and Meteorological pre-processors	While AERMOD has land use variability only in terms of wind sectors centered at the meteorological station, ADMS4 has the ability to produce 2-D variabilityfor surface roughness only. In comparison, CALPUFF has full 2-D spatial variability for all surface parameters based on a grid (variability in surface roughness length, anthropogenic and soil heat flux, Bowen ratio and albedo).
	Gaussian plume models use a single station wind to characterize the entire modeling domain. These plume models cannot generally replicate the actual wind fields in complex meteorological zones, whilst CALPUFF, using a 3-D wind field generated by CALMET, gives more realistic results, particularly in its ability to simulate spatial variability in the flow fields in complex terrains. CALMET can also use Numerical weather models (such as MM5) as gridded prognostic wind fields, and adjusts these to account for terrain kinematic effects, slope flows and blocking effects. This provides details of the space and time variability of the meteorology in three dimensions within the modeling domain.
Dispersion	1) CALPUFF is a Lagrangian puff modeling system that can track the plume's trajectory both temporally and spatially 2) Can model non-uniform meteorological conditions within the modeling domain, and the effect of complex terrain features and terrain downwash through the use of 3-D wind flow fields 3) Can model complex chemical transformations including aerosol formation 4) Ability to handle regions of stagnation (calm hours with wind speeds of <0.5m/s), through adjusting puff release characteristics 5) CALPUFF has an overwater turbulence module and a Thermal Internal Boundary Layer (TIBL) algorithm to treat coastal fumigation.

3.6 CALPUFF Input Database

Emission factors constitute a significant source of uncertainty in air quality modeling, particularly those related to industrial facilities, where the emissions pattern is subject to temporal variations. This variability may be attributed to the age of the equipment and on their maintenance, which tend to be difficult to reflect in emission inventories (El-Fadel et al. 2009; 2001).In the absence of representative emission factors, ranges of internationally reported values are frequently considered, and adjusted to account for case-specific conditions (quality of raw material, processing and fuel types, etc.) (Whyatt et al. 2007). Emission rates (ER) (mass of pollutant per unit time) (Equation 5) are

then derived based on the EF (mass of pollutant per mass or volume of product) and the Activity rate (AR) (mass of product per unit time), taking into consideration the reduction R (%) associated with the presence of control equipment.

$$ER = AR \times EF \times (1 - \frac{R}{100}) \qquad (5)$$

Table 5 summarizes the ranges of emission rates (g/s) derived for the criteria pollutants (CO, NO_x, SO_2 and PM_{10}) (El-Fadel and Abi-Esber 2011). The range of USEPA emission factors (USEPA, 1994) was determined depending on the performance of control devices, fuel composition, and source operational characteristics. As such, efficiencies of PM_{10} control devices were considered to range between 90 and 99% for electrostatic precipitators, 95 and 99% for bag house filters, 75 and 95% for cyclones and 85 to 97% for wet scrubbers. PM_{10} emissions from storage, handling and transport of product were calculated separately and added to the final emission factor. In the context of emissions from fuel combustion, nitrogen and sulfur mass contents ranging from 0.5 to 0.6% and 2 to 3% (the used range of sulfur mass content was based on values collected during field interviews with the industries), respectively, were assumed for residual oil, whereas a sulfur mass content varying between 0.5 and 1% was assumed for distillate oil. CO emission factors were assumed to vary by up to a factor of 10. Average vehicle speeds ranging between 55 and 60 miles per hour were used to determine highway emissions.

On the other hand, the ranges of EEA emission factors (EEA, 2009) were calculated based on Tier 1 and 2 emission factors[3] and corresponding 95% confidence intervals. The emission factors, which are reported in g/ton of product, were multiplied by the size of production of individual industries using Equation 5to yield a g/s total emission rate. In cases where emission factors are reported in g/GJ of energy consumed, heat values of 29.3, 45.0 and 32.6 GJ/ton of gas oil, fuel oil or petcoke were used along with the industries' total process fuel consumption to compute emission rates. Whenever Tier 2 emission factors were used, emissions from storage, handling and transport of product were calculated separately and added to the final emission factor (this type of emissions is implicitly accounted for in Tier 1 emission factors). In the case of cement and lime and plaster production, 99, 95 and 90% reduction in minimum, average and maximum PM_{10} emission factors were considered because the EEA emission factors assume that only ESP control is in place while field interviews with the industries showed that bag house filters are also being used (El-Fadel *et al*., 2009). Similarly, 99, 95 and 80% reduction in minimum, average and maximum SO_2 emission factors from the chemical industry with sulfuric acid production were considered because the EEA emission factors do not assume any type of controls while a wet scrubbing process is reportedly in place (El-Fadel *et al*., 2009).

[3] Tier 1 emission factors assume an average or typical process description. Tier 2 emission factors are developed on the basis of knowledge of the types of processes and specific process conditions reducing thus the level of uncertainty.

Table 5. Spectrum of emission rates (g/s)

Emittant Source (see Figure 1)	CO		NO_x		SO_2		PM_{10}	
	EEA (min-ave-max)	USEPA (min-max)	EEA (min-ave-max)	USEPA (min-max)	EEA (min-ave-max)	USEPA (min-max)	EEA (min-ave-max)	USEPA (min-max)
Point sources								
Holcim (1 &2)	104.1-208.1-416.2	15.5-46.5	41.6-161.3-624.3	120.6-212.6	2.1-38.9-728.4	50.6-107.1	0.5-4.4-12.8	326.5-825.7
Holcim (3)	5.4-10.8-21.6	0.43-5.03	2.2-8.4-32.4	8.4-13.8	0.1-2-37.8	21.8-34.3	0.055-0.83-2.16	4.7-49.9
CimenterieNationale (CN)	72.7-145.4-290.7	26.44-52.9	29.1-112.7-436.1	152-229.6	1.5-27.2-508.8	74.4-137.9	0.607-9.54-27.9	494.9-1861.3
Seament (CMO)	2.9-5.8-11.7	0.4-1.4	1.2-4.5-17.5	2-6.6	0.06-1.1-20.4	1.32-2.3	0.001-0.007-0.03	12.9-31.9
Lime & Plaster Co. (L&P)	0.03-0.20-1.40	0.014-0.16	0.05-0.30-1.40	0.21-0.43	0.02-0.20-1.20	0.80-1.25	0.028-0.25-0.57	1-2
Mineral Oil Recycling Co. (MORC)	0.001-0.0017-0.002	0.001-0.01	0.002-0.005-0.01	0.05-0.05	0.000004-0.0004-0.0007	0.02-0.04	0.000007-0.0004-0.0001	0.0011-0.0011
Lebanon Chemicals Co. (LCC)	0.3-0.7-10	0.2-2.3	0.09-1.7-2.6	3.4-3.8	0.38-3.5-16.1	29.6-48.2	0.012-0.105-0.3	1.6-2.2
Area sources								
Holcim quarry	-	-	-	-	-	-	0.095-0.57-2.84	30.9-36.6
CN quarry	-	-	-	-	-	-	0.051-0.36-2.06	112.3-142.9
L&P quarry	-	-	-	-	-	-	0.00012-0.00061-0.00307	16.7-16.7
Line sources								
Highway	3.55-77.27-154.54	2472- 4172	0.31-7.73-13.91	618.15-726.33	0.0031-0.03-0.31	0.0062-0.011-0.012	0.0062-0.011-0.012	-

It is worth noting that when one emission rate was assessed for its representativeness, it was applied for all source categories (for example, when assessing EEA_{max} emission rate for a given pollutant, the EEA_{max} value for every source was used). From a regulatory and environmental justice perspective, this might mask the inter-variability between sources. While one emission rate might be reasonably assessed as representative, some sources might not be emitting as such. However, this was contextualized within the tendency to conservatively estimate emission rates, and further analyzed via the source apportionment approach to reflect on the likelihood of over/underestimation of source strengths.

The modeling domain selected for the study area is a 50km×50km grid with a cell size of 0.5km×0.5km centered at Chekka. The prognostic mesoscale model version 5 (MM5) was used as input for CALMET to generate the 3-D meteorological and micrometeorological fields. All other meteorological processing options were set to model default. As an example, Figures 5 and 6 show two of the CALMET generated meteorological parameters (among many others such as a 3-D temperature profile, surface roughness length, solar radiation, Monin-Obukhov length, etc.), namely the wind field and mixing height. Figure 5 depicts the significant spatial variability in the wind field during a typical winter day (January 2003), with a relatively low wind speed (<3m/s), and Figure 6 shows the transition between the overwater and overland mixing heights.

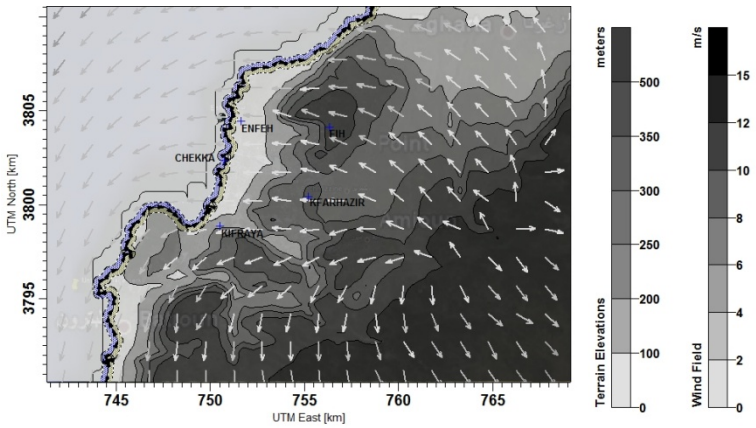

Figure 5. wind field (typical winter night-time, 10m height)

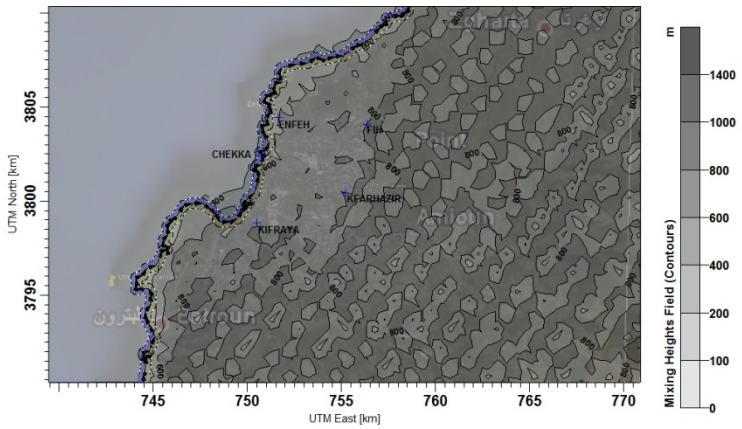

Figure 6. Mixing height field (winter daytime)

The effect of the land-sea interface was addressed through incorporating coastal fumigation in CALPUFF simulations. It was considered relevant to the study area as the sources are close to the coastline, and that such a transition in land use characteristics may affect plume dispersion, particularly plume trapping in the Thermal Internal Boundary Layer (TIBL). On the other hand, chemical transformations were not simulated due to lack of data on ambient concentrations of precursor gases (O_3, HNO_3, etc.) and other involved chemicals. However, such transformations are considered of less significance in such short-

range transport studies, with mild meteorological conditions that do not favor chemical reactions. Sensitivity of CALPUFF output to this assumption utilized the MESOPUFF II chemistry scheme within the model, where emissions of SO_2 and NO_x (NO and NO_2) are subject to first-order reaction mechanisms to form $(SO_4)^{2-}$ and $(NO_3)^-$ (nitrate aerosols) respectively, and thus decrease their ambient concentrations. The model defaults of ozone and ammonia background concentrations (80 ppb and 10 ppb respectively) were used, and considered to be uniform throughout the year.

CHAPTER 4

RESULTS AND DISCUSSION

4.1 Field Data Analysis

Field measurements are discussed in a context of preliminary data analysis and screening to identify any discrepancies, and summarized at each receptor to reflect on pollution levels within the study area. Table 6 shows the results for the gaseous pollutants (CO, NO_2 and SO_2) at each of the five locations throughout the whole year. Measurements for separate time periods at each location are presented later in this chapter in comparison to CALPUFF predictions.

Table 6. Summary of field measurements for gaseous pollutants

Parameter	CO			NO_2			SO_2		
Location (N_R)[a/]	Range ($\mu g/m^3$)	Mean ($\mu g/m^3$)	Exceedance[b/] (%)	Range ($\mu g/m^3$)	Mean ($\mu g/m^3$)	Exceedance (%)	Range ($\mu g/m^3$)	Mean ($\mu g/m^3$)	Exceedance (%)
Enfeh (939)	0-1336	172	0	0-188000	22600	64	0-5209	2900	63
Chekka (1032)	0-2237	598	0	0-38000	2200	85	0-1600	191	29
Fih (1081)	0-1630	541	0	0-185000	7600	83	0-4980	1090	24
Kfarhazir (1220)	0-1957	564	0	0-98000	2900	61	0	0	0
Kifraya (647)	0-2376	765	0	0-22000	1990	90	0-1480	87	18
EPA standards ($\mu g/m^{3)}$	1-hour avg=40000			1-hour avg=196			1-hour avg=196		

[a/]Total number of hourly records throughout the year
[b/]Percentage of hourly measurements exceeding the USEPA-NAAQS standards

CO levels were below the USEPA-NAAQS 1-hour average standard at all receptors, with Kifraya and Chekka witnessing relatively higher levels, being in close proximity to highway emissions. In contrast, NO_2 levels exceeded the standards at all monitored locations, with exceedance percentages ranging between 64% of the monitored

hours at Enfeh to 90% at Kifraya. The northerly receptors Enfeh and Fih witnessed significantly elevated peak values (*ca*. 188,000 µg/m^3) and averages, which is consistent with the prevailing Northerly to North-Westerly winds in the area. The lower mean concentration at Kfarhazir (2,900 µg/m^3) indicates that the peaks at this receptor (98,000µg/m^3) could be attributed to singular events rather than a dominant pattern. SO_2 peak and mean concentrations were highest at Enfeh and Fih, with the former showing higher exposure risk (exceedance for 63% of the times). Kfarhazir and Kifraya receptors were relatively safe, despite the infrequent exceedance of the standards at Kifraya (18% of the times).

Table 7 shows similar analysis for PM_{10} with highest concentrations (peaks and exceedance percentage) recorded at the close receptors, Chekka and Kifraya which is consistent with the fact that the range of PM_{10} transport is often shorter than that of gaseous pollutants due to gravitational settling associated with their heavier weight. Kfarhazir witnessed similar PM_{10} levels, which could be attributed to quarrying activities surrounding its perimeter.

Table 7. Summary of field measurements for PM_{10}

Parameter	PM_{10}			
Location	N_R (days)	Range (µg/m^3)	Mean (µg/m^3)	Exceedance (%)
Enfeh	7	60-170	110	14
Chekka	14	50-450	210	57
Fih	8	20-170	100	16
Kfarhazir	7	75-230	150	42
Kifraya	6	75-290	150	40
EPA standard (µg/m3)	24-hour avg= 150			

4.2 Estimation of Emission Rates

Each emission rate of the defined range was assessed for its proximity to the actual emissions in the study area under all circumstances. As such, simulations were conducted at all receptors and time periods using one emission rate (13 simulations at each emission rate), and statistical analysis of predictions against observations was carried out to reflect on the degree of matching between these datasets. This approach is intended to provide a statistically valid assumption of the representativeness of a certain emission rate (Lindley et al. 1996; Rege and Tock 1996). The results are presented on a pollutant-based segregation for CO, NO_2, SO_2 and PM_{10} respectively.

4.2.1 Carbon Monoxide (CO)

Table 8 summarizes the statistical analysis of CALPUFF performance at each CO emission rate, with values reflecting satisfactory correlations highlighted in bold. The statistical parameters indicate that simulations conducted using EEA_{max} exhibited best correlations at most receptors during different periods of the year. At Enfeh and Chekka, CALPUFF predictions using EEA_{max} matched observations closely (FB of -0.04 and 0.48 respectively when data were aggregated), with good correlations in MG, NMSE and FAC2. Simulations using EEA_{min} always under-predicted the observed mean concentration ($1.79 \leq FB \leq 2$), with weak correlations in other performance measures.

Table 8. Statistical analysis of CALPUFF predictions against observations for CO

Emission rate		EEA_{min}				EEA_{avg}				EEA_{max}				EPA_{min}				EPA_{max}			
Location	Time[a]	FB	MG	NMSE	FAC2(%)	FB	MG	NMSE	FAC2(%)	FB	MG	NMSE	FAC2(%)	FB	MG	NMSE	FAC2(%)	FB	MG	NMSE	FAC2(%)
Enfeh	Jan01-Jan11	1.83	21.8	30	5	1.13	4.4	3.5	16	**0.57**	**2.3**	**1.7**	**28**	-1.5	0.35	27.3	30	-1.7	0.2	47.6	27
	Apr19-May13	1.94	155	76	1	1.6	27.4	9	7	1.2	15	4	15	-1	2	9.5	24	-1.3	1.3	17	21
	Sep09-Oct05	1.76	6.2	41	23	**0.15**	**0.9**	**4.5**	**25**	**-0.5**	**0.51**	**6**	**26**	-1.9	0.06	123	19	-1.9	0.03	209	16
	Aggregate	1.81	11.3	41	16	0.63	2.2	4.12	20	**-0.04**	**1.2**	**4**	**24**	-1.75	0.16	79	20	-1.85	0.1	134	19
Chekka	Jan11-Feb02	1.92	63	55	2	1.06	7	2.6	18	**0.48**	**3.6**	**1.5**	**30**	-1.61	0.36	26	25	-1.76	0.22	45	16
	May13-May20	1.8	31	23	6	0.65	3.6	1.8	24	**-0.02**	**1.8**	**1.2**	**30**	-1.74	0.18	32	13	-1.84	0.1	56	12
	Sep06-Sep23	1.97	235	163	0	1.6	27	9	6	1.2	15	4	16	-1.1	1.7	9	20	-1.4	1.1	16	16
	Aggregate	1.92	63	55	2	1.06	7	2.6	14	**0.48**	**3.7**	**1.5**	**24**	-1.61	0.37	26	20	-1.76	0.23	45	16
Fih	Feb03-Feb19	1.98	298	210	1	1.94	190	66	1	1.88	156	34	1	1.12	81	4.8	5	0.71	67	5	7
	June15-July05	1.97	288	128	0	1.9	134	36	0	1.7	90	17	2	0.74	35	4.4	8	0.25	26	6.2	12
	Aug26-Sep06	1.86	24	45	13	1.52	7.7	10.4	13	1.1	4.6	4.7	18	-0.84	1.5	11.6	20	-1.22	0.98	19.8	21
	Aggregate	1.96	166	121	3	1.86	79	32.8	3	1.73	56	15.9	5	0.48	22.5	5.5	10	**-0.04**	**16.9**	**8.2**	**13**
Kfarhazir	Mar01-Mar15	1.92	35.2	66.5	10	1.28	8.2	5.7	14	**0.78**	**5**	**3.1**	**18**	-1.45	0.95	23	12	-1.66	0.64	39	15
	July05-Aug16	1.95	227	92	1	1.68	62.5	12.4	6	1.4	39	5.8	11	-0.75	8.3	15.4	15	-1.15	5.75	26.7	18
	Aggregate	1.94	135	89	3	1.6	35.5	10.5	8	**1.2**	**22**	**5**	**12**	-0.98	4.6	16.3	14	-1.33	3.1	28	16
Kifraya	Mar15-Mar23	1.86	50	31.7	1	**0.3**	**2.3**	**4**	**27**	**-0.4**	**1.1**	**6**	**41**	-1.84	0.07	124	5	-1.91	0.04	210	1
	June15-July05	1.79	51.3	22	2	**-0.2**	**2.6**	**22**	**30**	**-0.7**	**1.2**	**26**	**29**	-1.89	0.08	725	9	-1.94	0.05	1000	4
	Aggregate	1.8	51	25	2	**-0.1**	**2.5**	**23**	**30**	**-0.7**	**1.2**	**30**	**33**	-1.89	0.08	768	8	-1.93	0.04	1200	3

Also, EPA_{min} and EPA_{max} simulations over-predicted the mean concentrations (factors of 20 over-prediction, on average) at all receptors, except at Fih, where statistical measures calculated with EPA_{max} showed better performance. EEA_{avg} simulations generally under-predicted observations, with comparable performance to EEA_{max} at Kifraya only and for one period at Enfeh (Sep09-Oct05).

A most representative emission rate for CO was selected out of the defined range, based on a comprehensive statistical approach to the results in Table 8. As such, the statistical parameters (FB, MG, NMSE, and FAC2) calculated for each emission rate (Table 8) were averaged, and a range for the mean was defined based on 95% confidence intervals. This is intended to provide an overall assessment of the representativeness of each emission rate. Table 9 summarizes the results of this approach.

Table 9. Range of the mean for statistical indicators based on 95% confidence intervals (CO)

Emissions Parameter	EEA_{min}	EEA_{avg}	EEA_{max}	EPA_{min}	EPA_{max}
FB	1.89±0.03	1.09±0.32	**0.6±0.4**	-1.1±0.44	-1.32±0.37
MG	106.2±45.2	33.5±24.3	23±18	10±9.36	7±7.6
NMSE	73±24.4	14.4±7.63	**9±4.8**	112.8±107.3	173±159.3
FAC2(%)	5±3	15±5	**21±5**	15±3	14±3

The above discussion shows that CALPUFF predictions closely matched observations most frequently and at several locations when using EEA_{max}, which thus best represents CO emissions in the study area. Figure 7 shows the contribution of each source category to CO emissions, as approximated by the derived emissions rates EEA_{max} and EPA_{max}. The total CO emissions estimated by EEA_{max} is around 913 g/s, with highway emissions accounting for around 19% (170g/s), and point sources for 81% (743g/s).

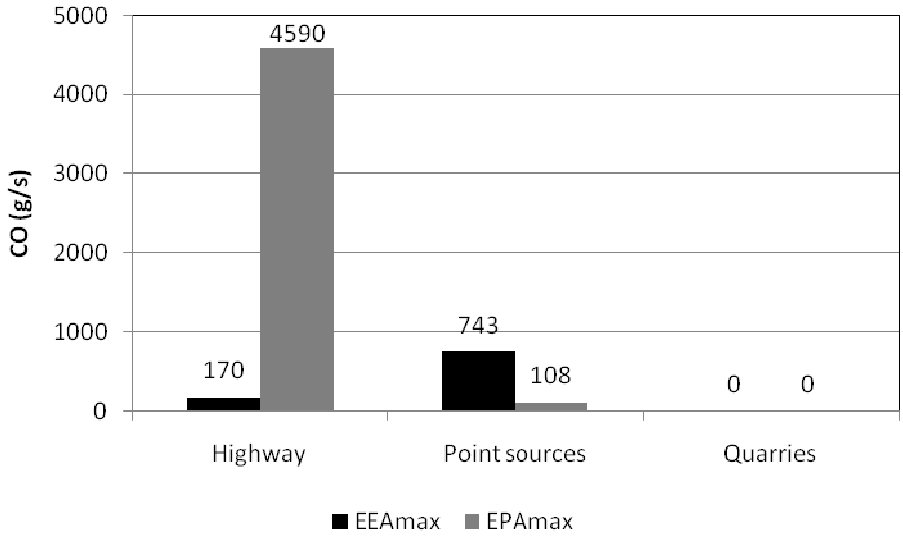

Figure 7. Contribution of source categories to CO emissions using EEA_{max} and EPA_{max}

On the other hand, EPA_{max} resulted in significantly higher total CO emissions (*ca*. 4700 g/s), with highway emissions accounting for 97%. This variability might explain the over-predictions of CALPUFF when EPA-based emission rates were used, particularly at receptors close to the highway (Enfeh, Chekka, and Kifraya). At Fih, which is the farthest receptor from the sources (≈7km), the prevalence of other sources to CO emissions is more probable (sources unaccounted for in CALPUFF simulations), given that it is a residential area (open burning, residential heating, arterial roads, etc.), and thus CALPUFF needs a higher-than-actual emission rate (EPA_{max}) to predict the mean.

4.2.2 Nitrogen Oxides (NO_x)

Table 10 shows the results of the statistical analysis performed for NO_2 predictions using all emission rates. The EEA-based emission rates (EEA_{min}, EEA_{avg}, and EEA_{max})

revealed weak correlations with observations, with under-prediction of the mean concentration (FB>1.9), and high values of NMSE and MG. The high FAC2 values (italic in Table 10) resulted from the fact that observations comprised a considerable number of low values which were replaced by the instrument's Limit of Quantitation (LOQ), and thus EEA predictions, which were also low values, matched this part of the dataset. On the other hand, the EPA-based estimations of the emission rates showed relatively better agreement with observations, particularly at Chekka (a factor of two under-prediction of the mean, on average), and Kifraya (a factor of two over-prediction, on average). However, these emission rates, despite better matching of observations than EEA rates, showed weak correlations at Enfeh, Fih and Kfarhazir, always with under-predictions. Overall, there is a tendency towards under-predictions when using those EPA-based emissions, except at Kifraya, which is the closest receptor to the center of sources (LO5 in Figure 1). The statistical parameters were also averaged for all simulations, and a range for the mean value was calculated based on 95% confidence intervals. Table 11 summarizes the results of this performance assessment.

Table 10. Statistical analysis of CALPUFF predictions against observations for NO_2

Emission rate		EEA_{min}				EEA_{avg}				EEA_{max}				EPA_{min}				EPA_{max}			
Location	Time	FB	MG	NMSE	FAC2(%)	FB	MG	NMSE	FAC2(%)	FB	MG	NMSE	FAC2(%)	FB	MG	NMSE	FAC2(%)	FB	MG	NMSE	FAC2(%)
Enfeh	Jan01-Jan11	No observations																			
	Apr19-May13	2	675	>1000	17	2	236	>1000	7	2	134	>1000	8	1.96	14	300	8	1.9	11.7	200	9
	Sep09-Oct05	2	58.6	>1000	*35*	1.98	20.5	980	21	1.95	12.2	418	20	1.12	1	16.7	19	**1**	**0.9**	**14**	**19**
	Aggregate	2	190.5	>1000	20	2	66.5	>1000	15	2	38.7	>1000	15	1.89	3.7	211	15	1.8	3	170	15
Chekka	Jan11-Feb02	2	182	>1000	21	1.97	33.8	463.6	5	1.96	49.5	397	12	0.7	1.2	7.25	17	**0.55**	**1**	**6.2**	**19**
	May13-May20		No observations																		
	Sep06-Sep23	2	>1000	>1000	1	1.98	388	177	1	1.95	226	79	1	0.99	14.6	1.9	22	**0.86**	**12.6**	**1.6**	**26**
	Aggregate	2	487	>1000	10	1.97	102	369	3	1.96	99	240	6	0.82	3.7	5.4	19	**0.67**	**3.1**	**4**	**22**
Fih	Feb03-Feb19	1.99	836	733	1	1.99	670	330	1	1.97	600	120	1	1.87	299	30	4	1.8	200	24	7
	June15-July05	2	>1000	>1000	12	2	763	>1000	9	1.98	485	>1000	8	1.98	234	516	7	1.97	204	420	8
	Aug26-Sep06	1.99	27	>1000	*39*	1.97	13	470	28	1.9	6.7	136	22	1.67	2.6	40	20	1.6	2.1	32.7	19
	Aggregate	2	451	>1000	11	2	291	>1000	10	1.98	200	>1000	8	1.95	91.5	474	8	1.9	81	388	8
Kfarhazir	Mar01-Mar15	2	900	>1000	5	1.98	311	249	5	1.94	197	91	5	1.25	30	5.3	20	**1.1**	**25**	**4**	**21**
	July05-Aug16	2	38	>1000	*40*	1.98	18.8	>1000	33	1.94	12.1	413	31	1.58	2.2	50	23	1.5	1.9	41	24
	Aggregate	2	92	>1000	*30*	1.98	41	>1000	25	1.94	26.4	352	22	1.5	4.6	35	22	1.4	3.9	29	22
Kifraya	Mar15-Mar23	2	100	>1000	27	1.92	9.2	208	1	1.86	5	114	1	**-0.41**	**0.1**	**8**	**33**	**-0.58**	**0.1**	**9**	**31**
	June15-July05	1.99	>1000	450	0	1.81	65	19.3	1	1.67	35	10.6	3	-1.17	0.9	74	35	-1.2	0.8	88	31
	Aggregate	1.99	696	813	7	1.84	38	36	1	1.71	20.6	20	3	-1.07	0.5	71.5	34	-1.1	0.44	85	32

Table 11. Range of the mean for statistical indicators based on 95% confidence intervals (NO_2)

Emissions Parameter	EEA_{min}	EEA_{avg}	EEA_{max}	EPA_{min}	EPA_{max}
FB	2±0.0	1.96±0.03	1.92±0.05	1.04±0.51	**0.9±0.5**
MG	364±159	192±117	134±87	44±44	**32±32**
NMSE	665±93	330±136	199±77	115±83	**94±66**
FAC2(%)	17±7	10±5	10±5	19±5	**20±4**

The EPA-based emission rates appear to better represent NO_x emissions in the study area, particularly EPA_{max}, at which CALPUFF predictions showed better agreement with observations. Figure 8 shows the contribution of each source category to total NO_x emissions as estimated by EEA_{max} and EPA_{max}. While both rates estimate comparable total emissions (1,130g/s and 1,266g/s respectively), the distribution among the source groups is different. Highway emissions account for only 1.3% (15 g/s) of total NO_x emissions when using EEA_{max}, but for 63% of total emissions when using EPA_{max}. The low weight assigned to Highway emissions in EEA_{max} is likely to have caused the under-predictions of the NO_2 concentrations (Table 10). Thus, and as a starting point, EPA_{max} is judged as more representative of NO_x emissions in the study area.

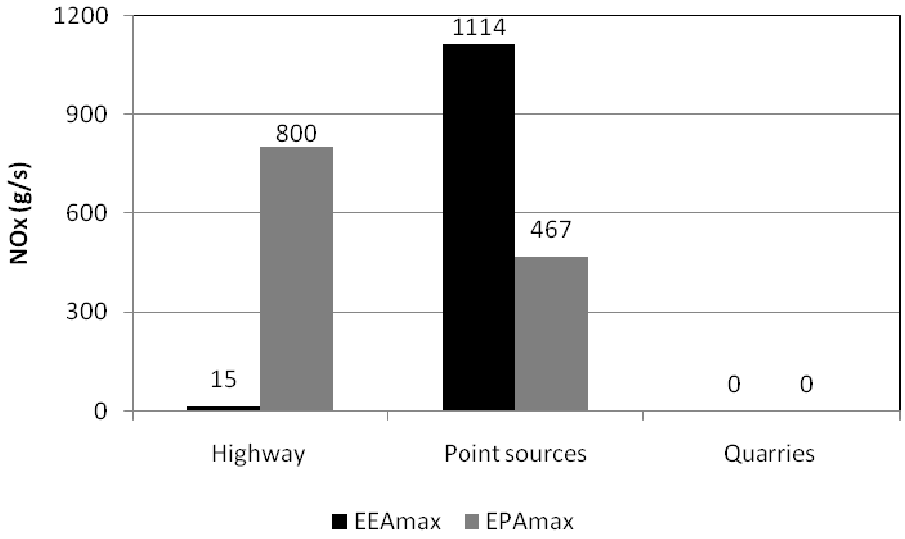

Figure 8. Contribution of source categories to NO_x emissions using EEAmax and EPAmax

4.2.3 Sulfur Dioxide (SO_2)

The measured concentration of SO_2 at most receptors and time periods was nil (see Table 12), except at Enfeh (Sep09-Oct05), Chekka (Sep06-Sep23), Fih (Aug26-Sep06) and Kifraya (June15-July05), reflecting higher pollution levels during summer times. It is worth noting that at periods where measured SO_2 concentrations were zero, CALPUFF predictions were also as such, but at all emission rates, and thus none of these could be judged as preferential. Tables 12 and 13 show CALPUFF performance measures at each emission rate during the periods of non-zero observations. All emission rates under-predicted the observed SO_2 concentration, with weak correlations between predictions and observations, allowing for no preferential selection.

Table 12. Statistical analysis of CALPUFF predictions against observations for SO_2

		EEA_{min}				EEA_{avg}				EEA_{max}				EPA_{min}				EPA_{max}			
	Time	FB	MG	NMSE	FAC2(%)	FB	MG	NMSE	FAC2(%)	FB	MG	NMSE	FAC2(%)	FB	MG	NMSE	FAC2(%)	FB	MG	NMSE	FAC2(%)
Enfeh	Jan01-Jan11	No observations																			
	Apr19-May13	No observations																			
	Sep09-Oct05	2	>1000	>1000	1	2	>1000	>1000	1	1.98	870	215	1	1.9	>1000	765	1	1.99	>1000	480	0
	Aggregate																				
Chekka	Jan11-Feb02	No observations																			
	May13-May20	No observations																			
	Sep06-Sep23	1.98	160	358	3	1.98	147	293	3	1.89	99	51	5	1.97	120	162	3	1.95	107	112	3
	Aggregate																				
Fih	Feb03-Feb19	No observations																			
	June15-July05	No observations																			
	Aug26-Sep06	2	>1000	>1000	0	2	>1000	>1000	0	1.95	455	83	0	1.99	>1000	550	0	1.99	850	316	0
	Aggregate																				
Kfarhazir	Mar01-Mar15	No observations																			
	July05-Aug16																				
	Aggregate																				
Kifraya	Mar15-Mar23	No observations																			
	June15-July05	1.93	9.7	196	46	1.92	8.7	151	46	1.5	4.3	22	35	1.85	6.9	84	45	1.79	6.13	56	45
	Aggregate																				

Table 13. Range of the mean for statistical indicators based on 95% confidence intervals (SO_2)

Parameter / Emissions	EEA_{min}	EEA_{avg}	EEA_{max}	EPA_{min}	EPA_{max}
FB	1.98±0.03	1.98±0.04	1.83±0.22	1.93±0.06	1.93±0.09
MG	542±521	539±524	356±350	534±529	491±489
NMSE	665±380	610±445	92±83	390±316	241±91
FAC2(%)	13±22	13±22	10±15	13±22	13±22

Both EPA_{max} and EEA_{max} attributed no SO_2 emissions to vehicles and quarrying sites (Figure 9). However, total SO_2 emissions estimated by each is different (1,312 g/s and 331 g/s by EEA_{max} and EPA_{max} respectively). Despite of this, CALPUFF predictions were comparable when using these rates, which reflect that the contribution of point sources to the SO_2 concentration at the monitored sites is insignificant, and thus highway SO_2 emissions were underestimated by both rates.

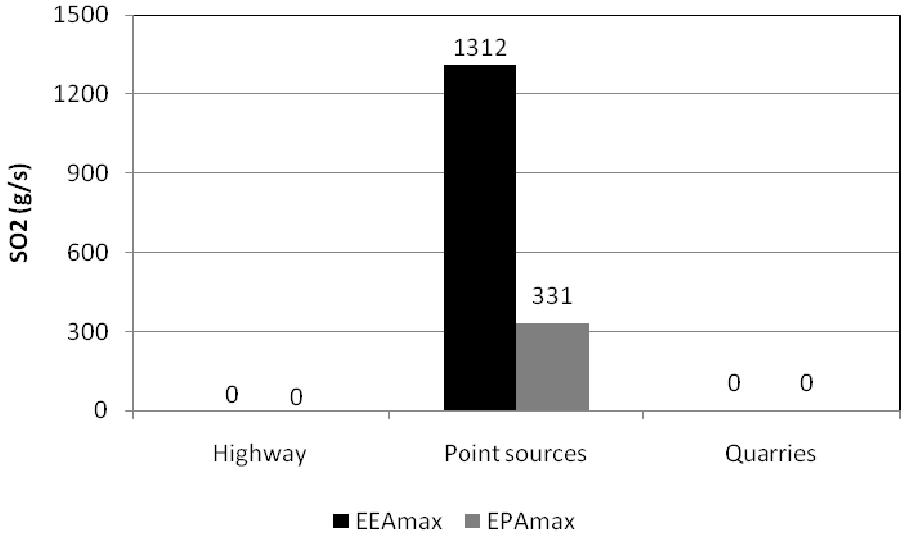

Figure 9. Contribution of source categories to SO_2 emissions using EEA_{max} and EPA_{max}

4.2.4 Dust (PM_{10})

Similar analysis conducted for PM_{10} (Table 14) indicates that CALPUFF under-predicted PM_{10} levels at all receptors and run periods when EEA-based emission rates were used, with low values of FAC2 and high values of MG and NMSE. EPA_{max} appears to be more representative of actual PM_{10} emissions, where CALPUFF predictions matched better observations at all receptors, with an FB as low as 0.09 at Enfeh and -0.01 at Fih, and slight over-predictions at Kfarhazir and Kifraya (FB = -0.21 and -0.56respectively). In an overall assessment, Table 15 further emphasizes that EPA_{max} is a better approximate to PM_{10} emissions in the study area, where CALPUFF revealed good performance in matching observed concentrations. Caution must be exercised when drawing conclusions from this particular analysis, as PM_{10} measurements were limited to discrete days only, and thus it is likely that the emitted plumes did not experience significant and statistically satisfactory meteorological variability that would allow legitimate inferences and assessments.

Table 14. Statistical analysis of CALPUFF predictions against observations for PM_{10}

		EEA_{min}				EEA_{avg}				EEA_{max}				EPA_{min}				EPA_{max}			
	Time	FB	MG	NMSE	FAC2(%)	FB	MG	NMSE	FAC2(%)	FB	MG	NMSE	FAC2(%)	FB	MG	NMSE	FAC2(%)	FB	MG	NMSE	FAC2(%)
Enfeh	Jan01-Jan11	1.96	26.5	252	18	1.94	17	148	18	1.85	8.2	56	14	**0.4**	**0.8**	**2.5**	**12**	**-0.67**	**0.33**	**2.1**	**22**
	Apr19-May13	1.97	102	194	0	1.97	94	173	0	1.96	83	126	0	1.3	18.6	6.1	14	**0.87**	**13**	**4**	**14**
	Sep09-Oct05	No measurements were made																			
	Aggregate	1.97	64.2	213.8	7	1.96	52.5	159.6	6	1.92	37	82.8	5	0.95	6.4	3.9	13	**0.09**	**3.7**	**2.6**	**17**
Chekka	Jan11-Feb02	2	>1000	>1000	0	1.97	357	284	0	1.92	128	97	0	0.37	2.7	2.9	4	**-0.16**	**1.7**	**2.8**	**20**
	May13-May20	2	>1000	>1000	0	1.9	>1000	650	0	1.9	>1000	181	0	1.34	119	4.1	13	**0.9**	**74**	**2.6**	**15**
	Sep06-Sep23	No measurements were made																			
	Aggregate	2	>1000	>1000	0	2	>1000	700	0	1.96	803	205	0	1.25	32.6	4.8	10	**0.85**	**20**	**3**	**17**
Fih	Feb03-Feb19	No measurements were made																			
	June15-July05	1.92	43.1	66.6	2	1.92	41	62.8	2	1.8	33.4	43	2	0.67	6.7	1.3	25	**-0.1**	**4.4**	**2.3**	**22**
	Aug26-Sep06	No measurements were made																			
	Aggregate																				
Kfarhazir	Mar01-Mar15	No measurements were made																			
	July05-Aug16	1.95	72	76	0	1.94	66	65	0	1.9	50	37	0	0.72	6	1.7	21	**-0.21**	**3.4**	**4.7**	**28**
	Aggregate																				
Kifraya	Mar15-Mar23	No measurements were made																			
	June15-July05	1.9	>1000	629	0	1.95	390	80	0	1.84	176	23	0	**0.22**	**7.2**	**2.5**	**13**	**-0.56**	**4.5**	**10**	**21**
	Aggregate																				

Table 15. Range of the mean for statistical indicators based on 95% confidence intervals (PM_{10})

Parameter / Emissions	EEA_{min}	EEA_{avg}	EEA_{max}	EPA_{min}	EPA_{max}
FB	1.96±0.02	1.95±0.02	1.89±0.03	0.8±0.28	**0.11±0.4**
MG	480±323	335±262	258±243	22±22	**14±14**
NMSE	490±270	258±161	94±42	3.3±1	**3.37±1.8**
FAC2(%)	3±3	3±3	3±3	14±4	**20±3**

Figure 10 shows the significant differences in total PM_{10} emissions estimated by EEA_{max} and EPA_{max} (EEA_{max}: 49 g/s; EPA_{max}: 2,970 g/s). However, both of these attribute no PM_{10} emissions to the Highway, and assign highest percentages to point sources out of the total (44g/s out of 49 for EEA_{max}, and 2,773g/s out of 2,970 for EPA_{max}), depicting then the significance of point sources in PM_{10} emissions and contribution to the ground level concentration at various receptors.

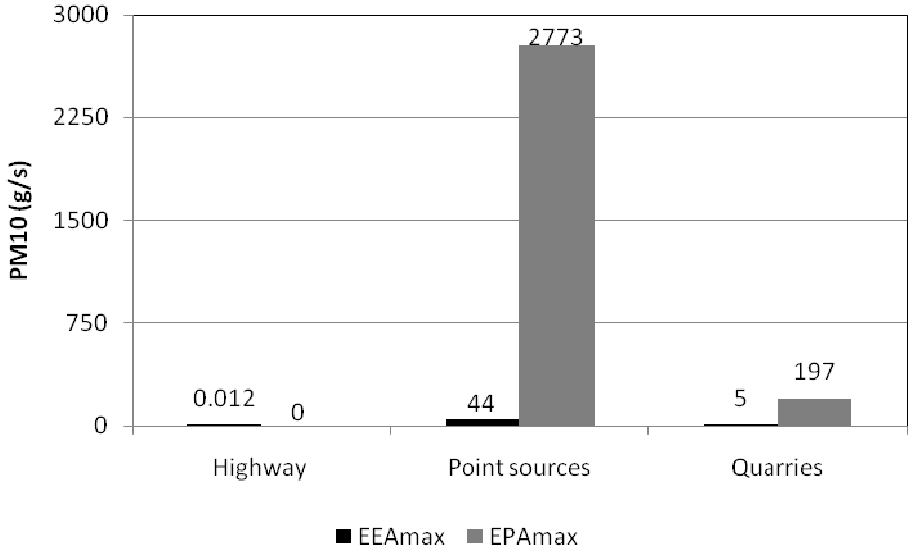

Figure 10. Contribution of source categories to PM_{10} emissions using EEA_{max} and EPA_{max}

4.3 CALPUFF Performance and Pollution Dimensions

The above discussion utilized CALPUFF in a predictive emissions scheme, where little consideration is given to its ability to predict more detailed features of the measured concentration field at the monitored locations. This was intended to help in the direction of selecting a most representative emission rate for each pollutant. While still considering the assumed emission rates as uncertain, the statistical parameters calculated in the previous discussion show a good performance of CALPUFF in predicting the mean concentration of various pollutants (except for SO_2), along with its ability to reproduce the scatter around this mean. In this section, CALPUFF is evaluated on its ability to reproduce other important features in the measured concentration dataset, particularly from a regulatory perspective. As such, CALPUFF predictions are examined in the context of how well they matched the higher ends of the concentration distribution (1^{st} highest 1-hour, 24-hour and 1-week averaging times), along with the index of agreement between the simulated and observed datasets. **.** The index of agreement reflects on how well model predictions reproduce variations around the observed mean concentration, and is used as a measure of the ability of the model to explain the potential for error in predictions. It ranges between 0 (no agreement between predictions and observations) and 1 (perfect agreement).Longer averaging times are relied upon mostly in regulatory contexts, as they mask the effects of unusual events that might lead to hourly outliers. Also, and to reflect on its ability to capture temporal fluctuations in the concentration, the number of predicted and observed peaks (defined as the number of measured concentrations above the mean of a dataset)is to be compared, along with time series and Q-Q plots. However, and as the American Society

of Testing and Materials (ASTM) points out, it is often fruitless to pair data in space and time to evaluate a model, as small fluctuations in the wind direction (5 to 10 degrees) might lead to no-overlap between the simulated and observed plumes, and thus the model may over/under-predict the concentration by 20 to 50% (ASTM 2000). As such, little regard is given as to whether CALPUFF predicted a peak concentration at the same time it occurred. Moreover, and to reflect on the pollution magnitude in the study area, these peak concentrations are compared to the USEPA-NAAQS primary standards for various pollutants (USEPA 2011).

The performance of CALPUFF is evaluated under different terrain and meteorological settings, and thus a receptor-based segregation is employed. At each receptor, CALPUFF predictions were evaluated at two time periods in an attempt to examine the effect of different meteorological conditions at this receptor on model performance. Equally important, this receptor-based segregation allows for a comparative assessment of performance under flat terrain setting (Enfeh and Chekka) and relatively complex terrain setting (Kifraya, Kfarhazir, and Fih). Note thatEEA_{max} is assumed to represent emissions of CO and SO_2, and EPA_{max} represents those of NO_x and PM_{10}.

Tables 16-20 summarize the results of the comparative assessment of predictions with observations at each location. CALPUFF predictions of the CO concentration distribution exhibited good agreement with observations at Enfeh, Chekka and Kfarhazir (Tables 16, 17 and 19). The highest predicted 1-hour and 24-hour average concentrations matched closely with their corresponding observations. At Chekka, CALPUFF estimated a

comparable highest 1-hour average CO concentration during a different time period of the year. The highest indices of agreement were 0.53, 0.40 and 0.40 at Enfeh, Chekka and Kfarhazir respectively. Moreover, CALPUFF tended to underestimate the longer-time averages during summer times (May to September), which were characterized by non-uniform winds at the three sites, and lower average wind speeds compared to winter times (see Figure 11), leading to weaker dispersion and more near-source accumulation. The highest hourly CO concentrations at the three sites, both predicted and observed, are well below the 1-hour average USEPA-NAAQS standard, indicating no risk of exposure toelevated CO concentrations. At Fih and Kifraya, CALPUFF predictions showed weaker correlations, with under-predictions at Fih and over-predictions at Kifraya. Fih is the farthest receptor, lying to the North-East of the majority of the sources, and thus the uniform Northerly winds during winter (Feb03-Feb19)(Figure 11-e) and the low summer wind speeds (Figure 11-f) may explain such under-predictions. As for Kifraya, its proximity to the sources, particularly the highway, may result in higher CO concentrations, albeit less than the standards.

Table 16. CALPUFF performance at Enfeh

					1-hour averaging time				Longer-time averages		USEPA-NAAQS		
Receptor	Time period		N_R[a]	d[b]	Concentration[c] ($\mu g/m^3$)	1st highest	Mean	N_P[d]	Max. 24-hour avg	Max. 1-week avg	1-hour avg	24-hr avg	Percentage of exceedances (%)
Enfeh	Jan01-Jan11	CO	239	0.53	C_o	1025	311	112	426.8	274	40,000	-	0
					C_p	1153	174	75	400	110			0
		NO_2		-	C_o	Measurements were all zero					196	-	0
					C_p	5350	633	55	1849	1490			47%
		SO_2		-	C_o	Measurements were all zero					196	366.5	0
					C_p	287	73.5	80	169	101			1-hr:19%; 24-hr: 0
		PM_{10}	50=2days	0.43	C_o	443	126	20	231	-	-	150	50% : 1/2 days
					C_p	495	251	26	256	-			100% : 2/2 days
	Apr19-May13	CO	563	0.34	C_o	1336	570	340	747	630	40,000	-	0
					C_p	1325	130	201	396	140			0
		NO_2		0.44	C_o	188,140	43,857	180	155,767	95643	196	-	70%
					C_p	5700	504	172	1833	500			52%
		SO_2		-	C_o	Measurements were all zero					196	366.5	0
					C_p	1434	40	90	161	66			1-hr: 7% ; 24-hr: 0
		PM_{10}	95=4days	0.32	C_o	310	132	40	176	-	-	150	25% =1/4 days
					C_p	652	55	25	106	-			0

[a]Number of hourly records and the equivalent days
[b]Index of agreement
[c]C_o=Observed; C_p=Predicted
[d]Number of peaks (measurements exceeding the mean value)

Table 17. CALPUFF performance at Chekka

					1-hour averaging time				Longer-time averages		USEPA-NAAQS		
Receptor	Time period		N_R	d	Concentration ($\mu g/m^3$)	1st highest	Mean	N_p	Max. 24-hour avg	Max. 1-week avg	1-hour avg	24-hr avg	Percentage of exceedances (%)
Chekka	Jan11-Feb02	CO	480	0.40	C_o	1025	473	270	673	540	40,000	-	0
					C_p	2630	291	165	740	440			0
		NO_2		0.30	C_o	37,848	2228	146	8725	3000	196	-	73%
					C_p	11,785	1275	162	2942	1950			65%
		SO_2		-	C_o	Measurements were all zero					196	366.5	0
					C_p	817	23.4	113	70	35			1-hr: 2%; 24-hr: 0
		PM_{10}	25=1day	0.17	C_o	294	56	9	56	-	-	150	0
					C_p	299	65	10	65	-			0
	Sep09-Oct05	CO	401	0.36	C_o	2237	857	195	1298	1040	40,000	-	0
					C_p	1780	188	140	415	249			0
		NO_2		0.06	C_o	2288	2126	176	2173	2130	196	-	100%
					C_p	8355	853	130	2262	1137			61%
		SO_2		0.45	C_o	1597	498	185	942	612	196	366.5	1-hr:76% ;24-hr: 94%
					C_p	610	14	41	56	16			1-hr: 2% ; 24-hr: 0
		PM_{10}	-	-	C_o	No measurements were made					-	150	-
					C_p	1166	61	87	257	87			6%: 1/17days

Table 18. CALPUFF performance at Fih

					1-hour averaging time				Longer-time averages		USEPA-NAAQS		
Receptor	Time period		N_R	d	Concentration ($\mu g/m^3$)	1st highest	Mean	N_p	Max. 24-hour avg	Max. 1-week avg	1-hour avg	24-hr avg	Percentage of exceedances (%)
Fih	Feb03-Feb19	CO	366	0.27	C_o	1039	492	271	559	515	40,000	-	0
					C_p	250	16	62	63	22			0
		NO_2		0.28	C_o	2446	1109	172	1505	1085	196	-	100%
					C_p	984	45	70	175	45			7%
		SO_2		-	C_o	Measurements were all zero					196	366.5	0
					C_p	376	10	34	52	19			1-hr: 2%;24-hr: 0
		PM_{10}	50=2days	-	C_o	123	28	21	42	-	-	150	0
					C_p	166	11.5	6	22	-			0
	June15-July05	CO	470	0.31	C_o	1630	731	213	920	788	40,000	-	0
					C_p	580	41	130	180	95			0
		NO_2		0.36	C_o	184,830	15,600	137	34,300	23,990	196	-	85%
					C_p	2180	110	78	540	222			12%
		SO_2		-	C_o	Measurements were all zero					196	366.5	-
					C_p	648	35	105	128	53			1-hr: 5% ; 24-hr: 0
		PM_{10}	73=3days	0.53	C_o	263	101	19	139	-	-	150	33% =1/3 days
					C_p	1090	112	23	194	-			33% =1/3 days

Table 19. CALPUFF performance at Kfarhazir

					1-hour averaging time				Longer-time averages		USEPA-NAAQS		
Receptor	Time period		N_R	d	Concentration ($\mu g/m^3$)	1st highest	Mean	N_p	Max. 24-hour avg	Max. 1-week avg	1-hour avg	24-hr avg	Percentage of exceedances (%)
Kfarhazir	Mar01-Mar15	CO	340	0.37	C_o	1063	351	192	549	499	40,000	-	0
					C_p	1147	155	110	420	158			0
		NO_2		0.34	C_o	12,230	2390	152	3818	2608	196	-	93%
					C_p	5390	660	102	1860	680			40%
		SO_2		-	C_o	Measurements were all zero					196	366.5	0
					C_p	650	27	53	67	27			1-hr: 5%; 24-hr: 0
	July05-Aug16	CO	880	0.40	C_o	1957	646	421	939	700	40,000	-	0
					C_p	1954	113	212	560	201			0
		NO_2		0.28	C_o	97,880	3060	229	12,525	6490	196	-	49%
					C_p	9091	435	162	2435	685			27%
		SO_2		-	C_o	Measurements were all zero					196	366.5	-
					C_p	1164	42	137	188	78			1-hr: 8% ; 24-hr: 0
		PM_{10}	72=3days	0.09	C_o	216	149	34	164	-	-	150	67% =2/3 days
					C_p	2289	183	17	277	-			33% =1/3 days

Table 20. CALPUFF performance at Kifraya

					1-hour averaging time				Longer-time averages		USEPA-NAAQS		
Receptor	Time period		N_R	d	Concentration ($\mu g/m^3$)	1st highest	Mean	N_p	Max. 24-hour avg	Max. 1-week avg	1-hour avg	24-hr avg	Percentage of exceedances (%)
Kifraya	Mar15-Mar23	CO	183	0.07	C_o	916	415	88	477	410	40,000	-	0
					C_p	13,182	640	40	2765	675			0
		NO_2		0.24	C_o	22,200	1660	68	4380	1670	196	-	63%
					C_p	61,900	3000	40	5440	3100			100%
		SO_2		-	C_o	Measurements were all zero					196	366.5	0
					C_p	42	2	34	4	2			1-hr: 0%;24-hr:0

NO_2 predictions showed weaker correlations, with a tendency towards under-predictions of highest observed concentrations, except at Kifraya and Chekka (September), where CALPUFF overstated the observed maxima, but matched better the highest 24-hour and weekly averages. SO_2 and PM_{10} predictions were in good agreement with observations, with an average SO_2 concentration as low as 2 $\mu g/m^3$ when measurements were zero. All sites appear to be at ambient concentrations of NO_2, SO_2 and PM_{10} with high exceedance frequency to the standards, with CALPUFF predicting less exceedance percentage, except at Kifraya. The model's performance appears not to correlate to the terrain setting at the receptor, given a comparably satisfactory performance at Kfarhazir, for instance. However, CALPUFF tended to over-predict at sites very close to the sources, such as Kifraya. The high under-predictions at Fih, except for PM_{10}, could be attributed to underestimations of the contribution of elevated point sources, particularly that highway emissions are less likely to contribute to such relatively far receptors, or to the likelihood of the presence of other localized sources.

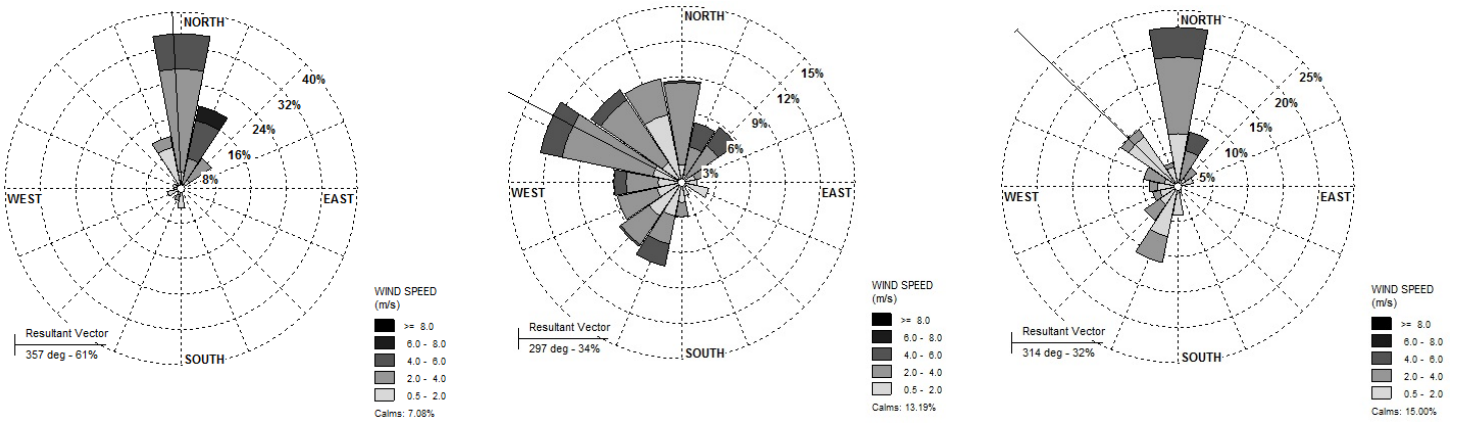

a- Enfeh (Jan01-Jan11)

b- Enfeh (Apr19-May13)

c- Chekka (Jan11-Feb02)

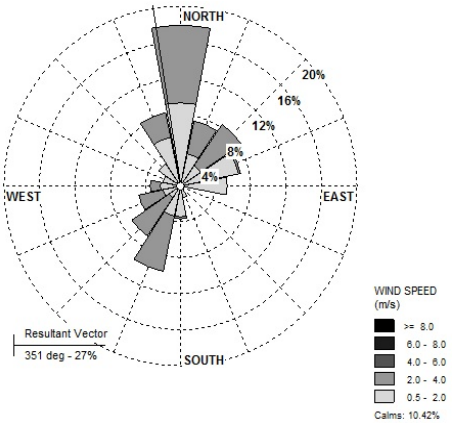

d- Chekka (Sep09-Oct05)

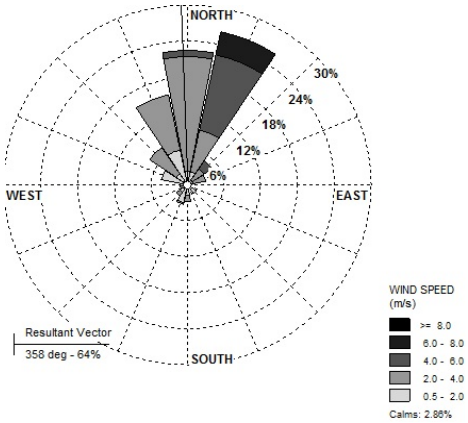

e- Fih (Feb03-Feb19)

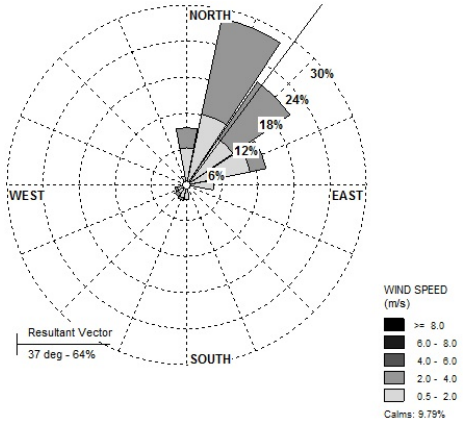

f- Fih (Jun15-Jul05)

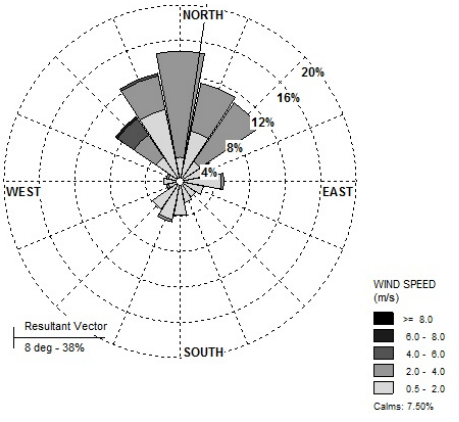

g- Kfarhazir (Mar01-Mar15)

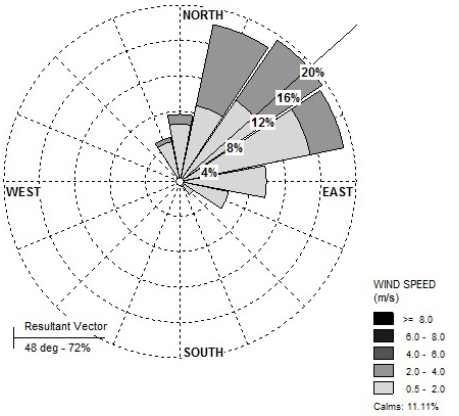

h- Kfarhazir (Jul05-Aug16)

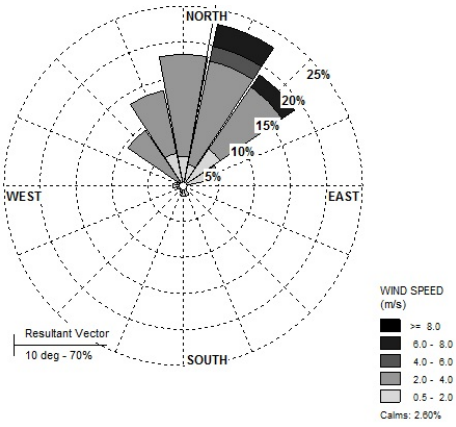

i- Kifraya (Mar15-Mar23)

Figure 11. Wind-roses at the monitored receptor locations (direction: blowing to)

For a visual inspection of such features, Figures 12 and 13 show the concentration time series for CO and NO_2respectively, at selected receptors and time periods. These plots are chosen for presentation brevity, and at locations where CALPUFF performed best in stating temporal trends in the observed concentration distribution. The simulated CO concentration field showed very good agreement with both the magnitude and temporal fluctuations in observations, particularly at Enfeh, Chekka and Kfarhazir, indicating that CALPUFF was able to reproduce the concentration pattern fairly well. However, and although the predicted concentration was comparable to observations most of the time at Kifraya, infrequent over-predictions are evident (Figure 12-e). Besides, CALPUFF generally under-estimated the CO concentration at Fih (Figure 12-f), but always with predictions lying within a factor of two of observations.

Similar analysis for the NO_2 predicted concentration further emphasizes good performance of CALPUFF at several locations (Figure 13), albeit the slight under-predictions at Kfarhazir (less than a factor of two, on average) (Figure 13-b) and Enfeh (less than a factor of five, on average) (Figure 13-d). Figure 14 shows selected time series and Q-Q plots for SO_2 and PM_{10} respectively, as examples. CALPUFF generally under-predicted the SO_2 concentration at Kifraya but showed excellent matching of the higher end of the PM_{10} concentration at Chekka.

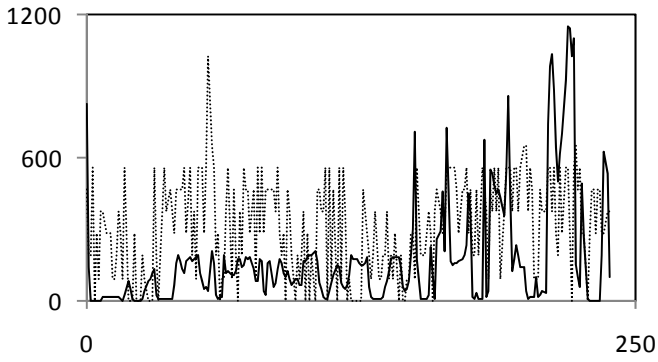

a- Enfeh (Jan01-Jan11)

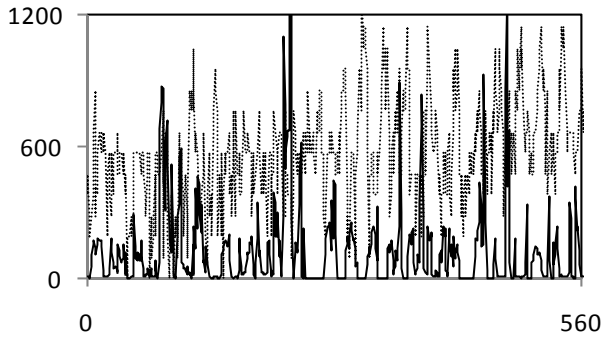

b- Enfeh (Apr19-May13)

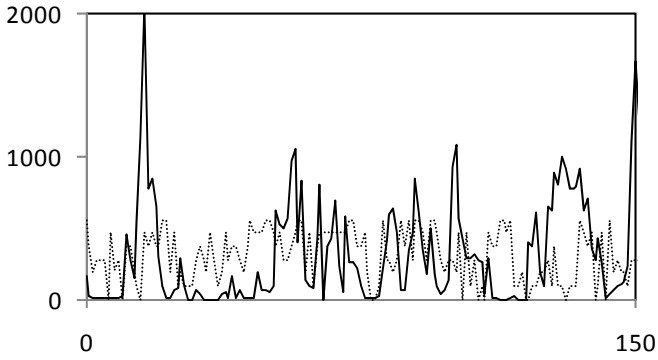

c- Chekka (May13-May20)

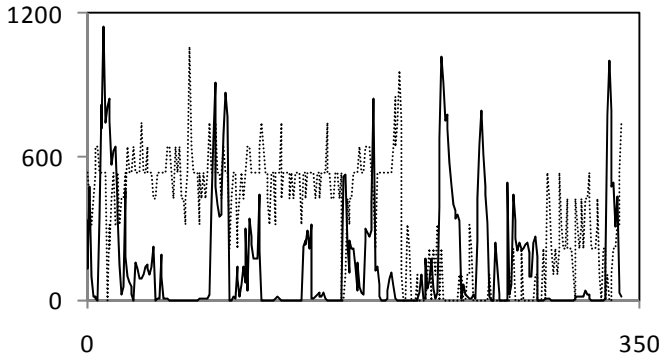

d- Kfarhazir (Mar01-Mar15)

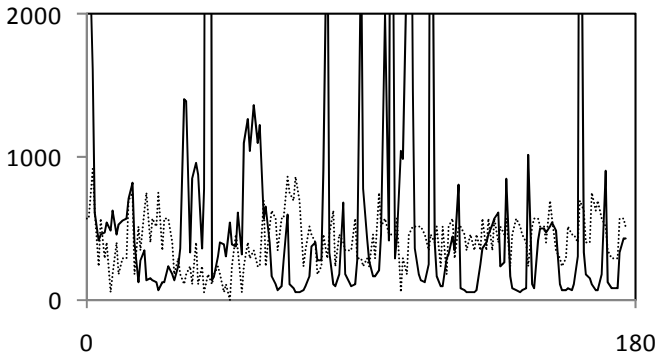

e- Kifraya (Mar15-Mar23)

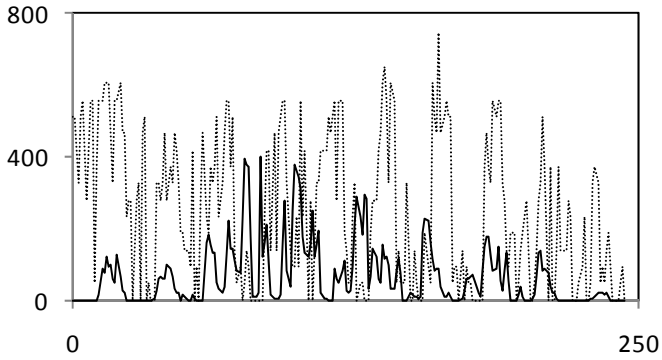

f- Fih (Aug26-Sep06)

Figure 12. Time series (hourly) of CO (µg/m^3) at various receptors

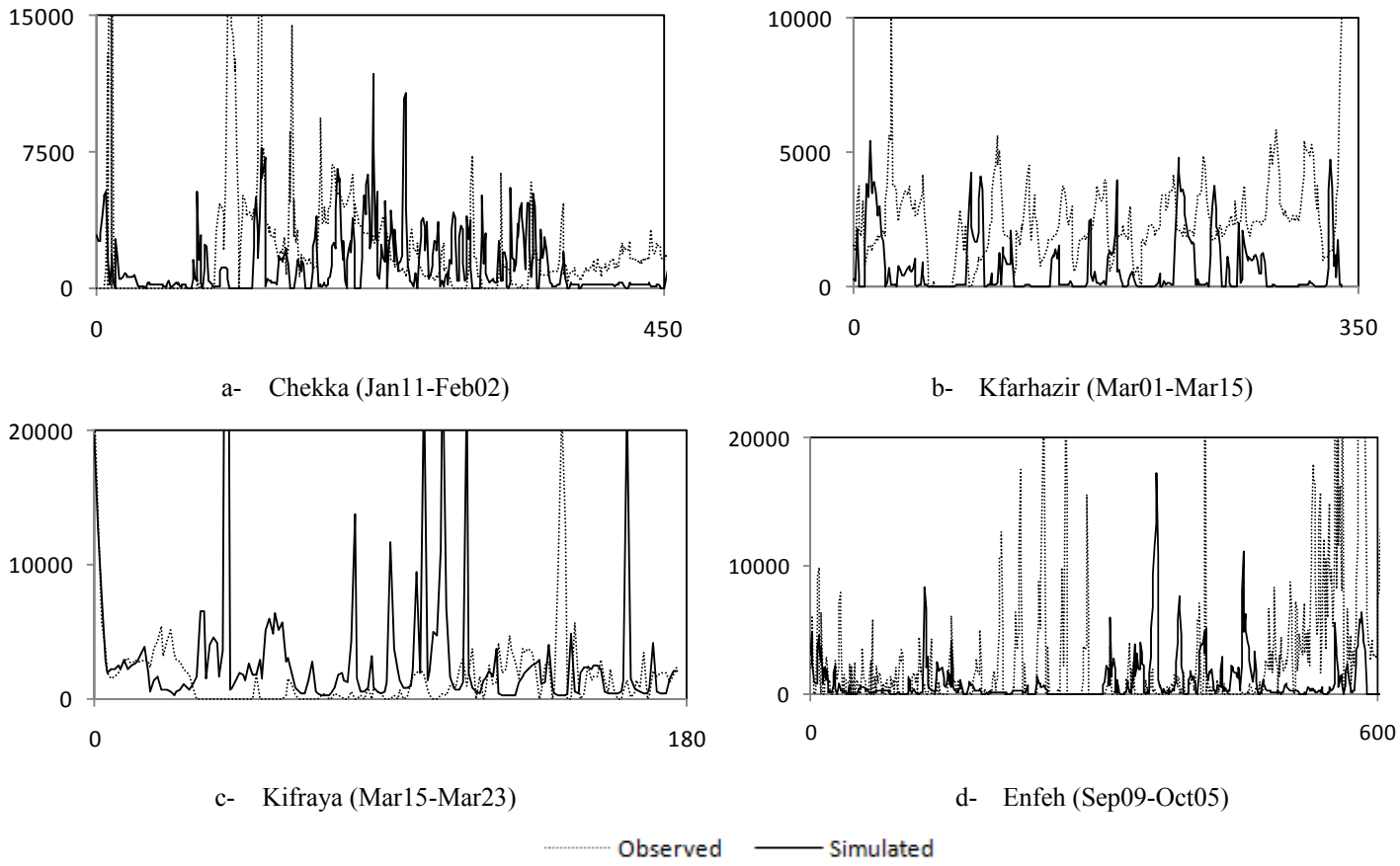

a- Chekka (Jan11-Feb02)

b- Kfarhazir (Mar01-Mar15)

c- Kifraya (Mar15-Mar23)

d- Enfeh (Sep09-Oct05)

Figure 13. Time series (hourly) of NO_2 (µg/m^3) at various receptors

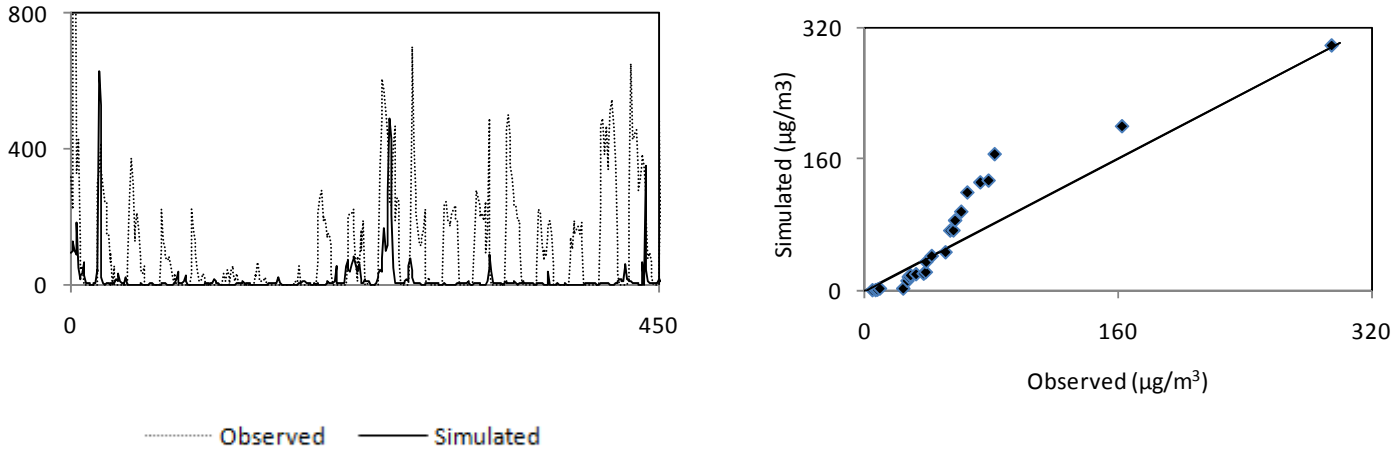

a- SO_2 (µg/m^3) at Kifraya (June15-July05)

b- PM_{10} (µg/m^3) at Chekka (24 hourly records)

Figure 14. a) Time series (hourly) of SO_2 at Kifraya. b) Q-Q plot for PM_{10} at Chekka

Although CALPUFF revealed variable performance at different locations and for different pollutants, it reproduced field measurements at the monitored locations reasonably well. However, the spatial distribution of the ground level concentration over the entire domain is of interest in regulatory contexts. In particular, regions of elevated concentrations (hot spots) of criteria pollutants, and the temporal variability of this distribution would assist in delineating vulnerable areas as a starting point for management scenarios. Given that the USEPA-NAAQS standards for CO and NO_2 are 1-hour averages, and those for SO_2 and PM_{10} are 24-hour averages (SO_2 1-hour average standard is avoided due to limitations related to hourly outliers associated with calm conditions), contour plots for these pollutants are shown in analogy with these averaging times.

Figures 15 and 16 show the spatial distribution of the highest ranks of concentrations during winter and summer times, respectively. While highest concentrations were frequently predicted at the same location for CO and NO_2,higher accumulations are noticeable during summer times, with a maximum reaching 174,000 $\mu g/m^3$for CO and 800,000 $\mu g/m^3$ for NO_2. A larger percentage of the total area is affected by elevated concentrations of the two pollutants during summer times, particularly near Kifraya, and to the south-east of the study area. However, CO concentration in the study area was lower than the 1-hour average standard (40,000 $\mu g/m^3$), except near Kifraya during summer times, while the NO_2 concentration exceeded the standard (196 $\mu g/m^3$) over the entire domain[4], with elevated concentrations near the source.

[4]UTM: Universal Transverse Mercator: grid-based geographic projection system in which Earth is divided into 36 UTM zones each with 6^0width. Lebanon lies in UTM zone 36N (Northern hemisphere)

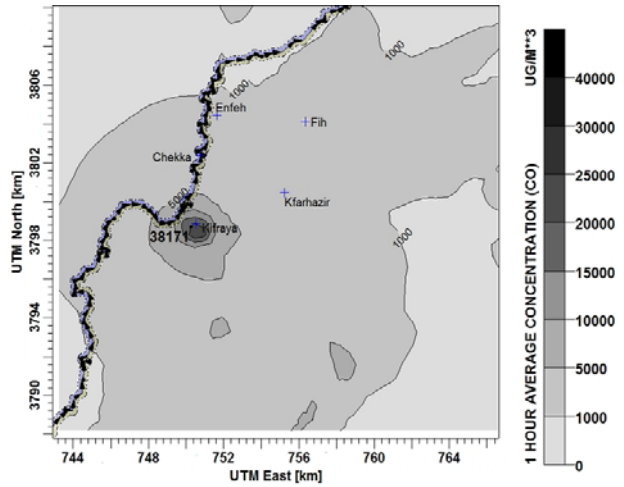

a- Highest 1-hour CO concentration (µg/m^3)

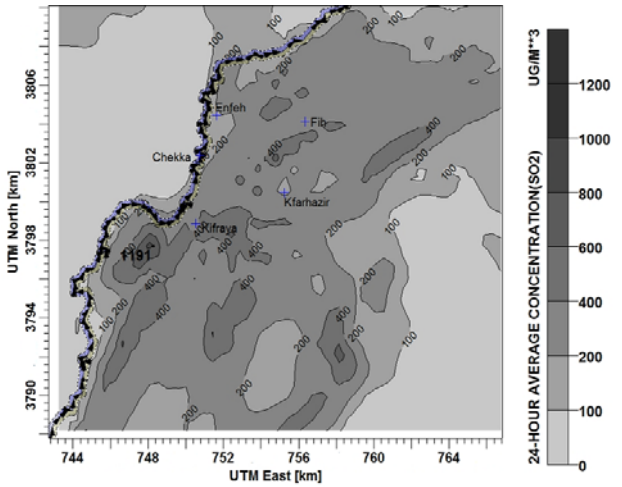

b- Highest 24-hour SO_2 concentration (µg/m^3)

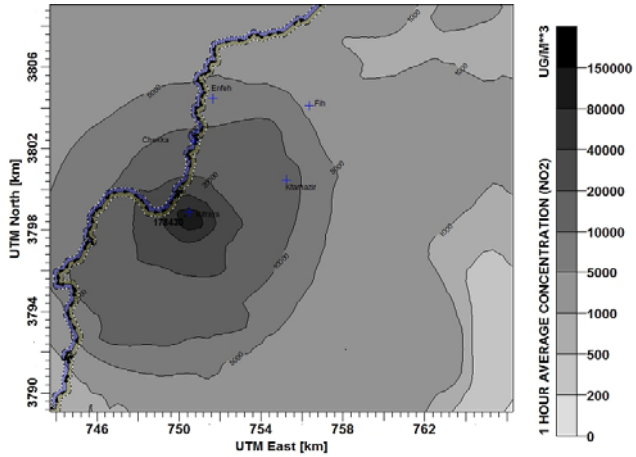

c- Highest 1-hour NO_2 concentration (µg/m^3)

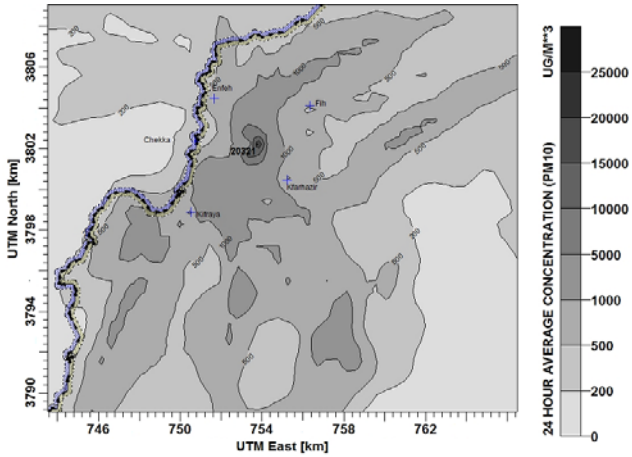

d- Highest 24-hour PM_{10} concentration (µg/m^3)

Figure 15. Spatial distribution of criteria pollutants concentration (January-winter times)

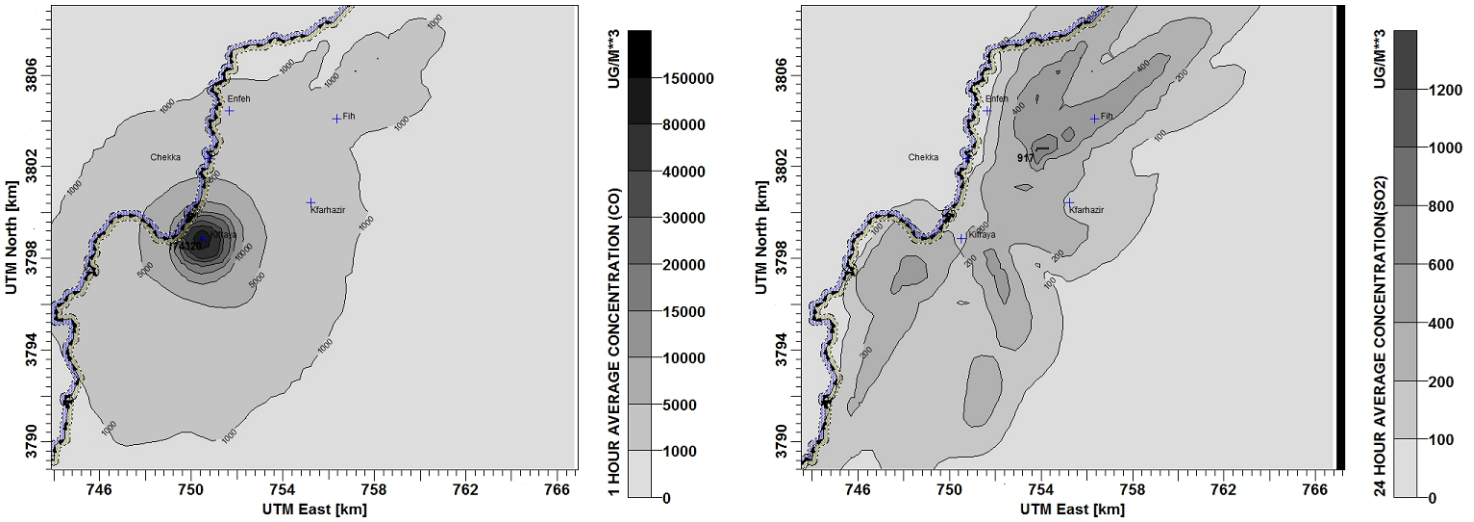

a- Highest 1-hour CO concentration (µg/m^3)

b- Highest 24-hour SO_2 concentration (µg/m^3)

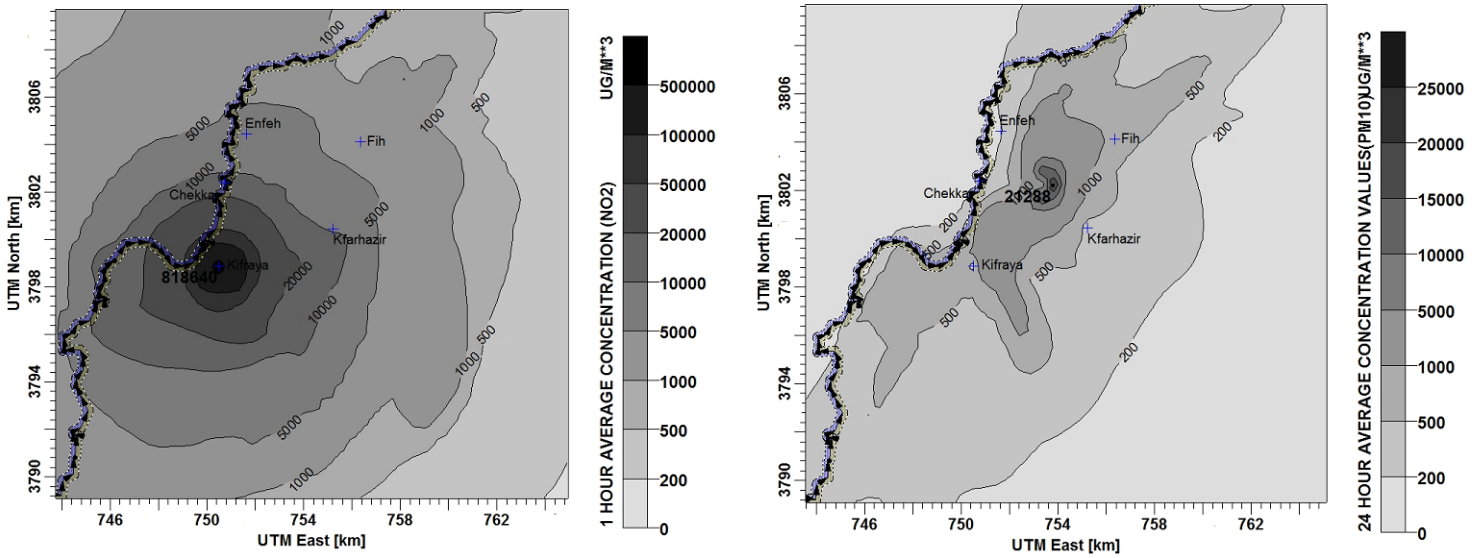

c- Highest 1-hour NO_2 concentration (µg/m^3)

d- Highest 24-hour PM_{10} concentration (µg/m^3)

Figure 16. Spatial distribution of criteria pollutants concentration (July/August-summer times)

As for SO_2 (Figure 15-b and 16-b), the highest concentration shifted towards the north-east during summer, with a slight decrease from around 1200 in winter to 917 µg/m^3 during summer. Also, and given that only point sources contribute to SO_2 emissions, the significant variability of the SO_2 concentration over the entire domain depicts the prevalence of each point source to the contribution at its neighborhood. Throughout the

whole year, the SO_2 concentration in the study region exceeded the 24-hour average standard (366.5 μg/m^3), particularly in winter times, where exceedance is noticed at a larger area of the region and with greater magnitude. PM_{10} concentration distribution (Figure 15-d and 16-d) reveals similar trends as CO and NO_2, with the highest concentration occurring frequently close to CN quarry, but with essentially no seasonal differences (*viz.* 20,000 and 21,200 μg/m^3 during winter and summer respectively), larger areas affected by elevated concentrations during summer times, and with concentrations exceeding the 24-hour average standard (150 μg/m^3) over most of the modeling domain.

4.4 Source Apportionment

The contribution of various source groups to pollutant concentration at different receptors is addressed in this section. This aims at identifying major contributors that need to be targeted for mitigation measures, and also to reflects on the uncertainty associated with the estimation of emission rates. Moreover, this approach allows for further analysis of CALPUFF performance, particularly the likelihoods of over/underestimations and thus explanations of why would CALPUFF perform in a certain manner. As explained earlier, the contribution of a particular source could be evaluated in two ways, “emissions in” and “emissions out” approaches. In brief, “emissions in” simulations consider the source of interest to be emitting only, and thus its contribution is the predicted concentration. On the other hand, “emissions out” simulations remove the emissions from that source, keeping all others, and the contribution of the source is the difference between the “base-case” predicted concentration (all sources emitting) and that of the “emissions out” simulations.

This tests if CALPUFF is summing the contribution of the various sources at a receptor, and reflects on its linear response to gross emissions. The following analysis relies on Carbon Monoxide (CO), as it is an inert gas, but the results are deemed valid for other pollutants, given that chemical transformations are not simulated, and further justified in the next section to be insignificant. Also, the contribution of sources is evaluated on long-time averages, particularly the maximum weekly average during a single period, and on time series of the 24-hour averages to provide a contribution assessment over finer temporal scales. Furthermore, one time period at each receptor is analyzed, namely those where CALPUFF showed best performance as these are considered the most reliable for such analysis.

Emissions of Carbon Monoxide are limited to two source categories, namely Highway and point sources. The contribution of Highway emissions was calculated through the "emissions in" simulations (EI), where the highway was considered to be emitting only, and through the "emissions out" (EO) simulations, where only point sources emissions are considered. Highway contribution in the latter approach was calculated through the difference between the "base-case" predicted concentration and the "emissions out" simulations. To test the linearity of CALPUFF, the ratio of the predicted 24-hour average concentration in the EI to that in the EO is shown in Figure 17 (a-d), at different receptors and time periods. It is worth noting that the same results could be generalized for all receptors, but only these are shown as examples.

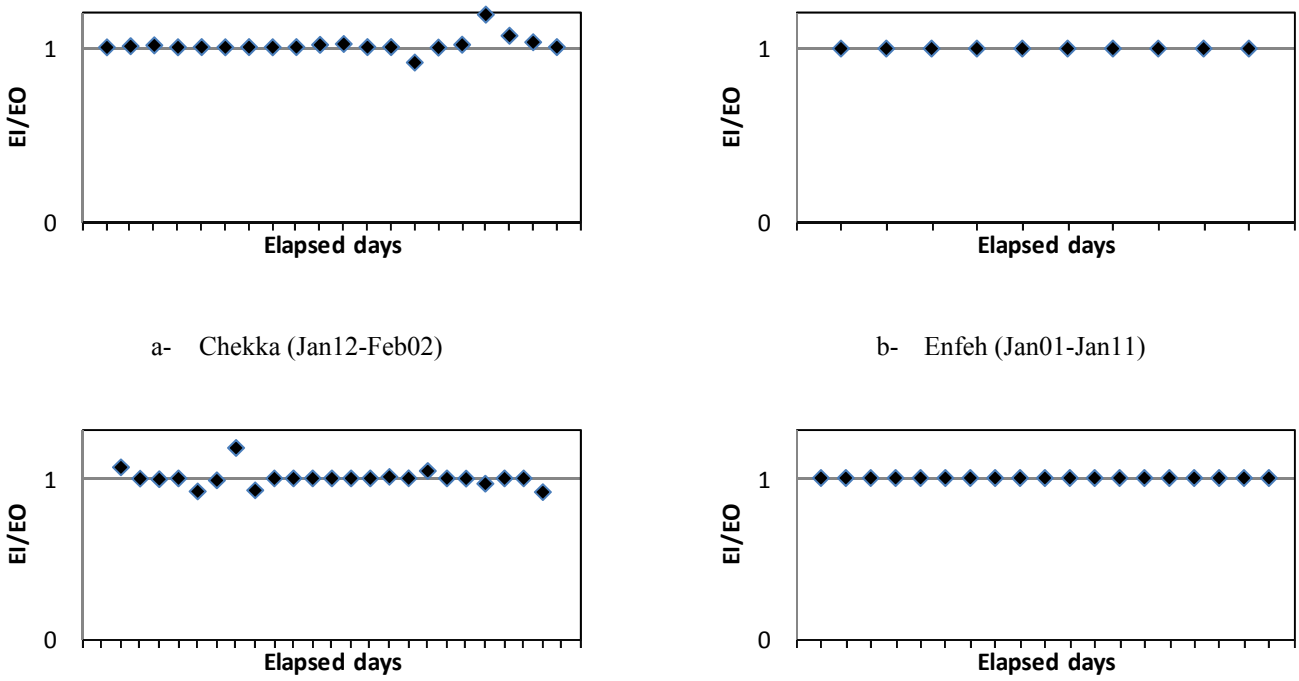

a- Chekka (Jan12-Feb02)

b- Enfeh (Jan01-Jan11)

c- Enfeh (Apr19-May13)

d- Fih (June15-July05)

Figure 17. Ratio of the 24-hour average CO concentration predicted via the EI and EO scenarios

Clearly, highway contribution to CO levels is equivalent in the two scenarios, with a ratio of EI/EO always unity, except for two days at Chekka (Figure 17-a) and three days at Enfeh (Figure 17-c), but with negligible deviation (0.9-1.2). It is worth noting that those days of over-prediction of the highway contribution (EI/EO>1) were characterized by higher wind speeds and less calms frequency, as opposed to days of under-predictions. For instance, the day with under-prediction at Chekka was characterized by high percentage of calm hours (11 out of 24) and low average wind speed (0.6 m/s), which may explain the underestimation of the highway contribution (EI/EO=0.9) during that day. Days of over-predictions however, were characterized by zero calm hours and high wind speeds (4.6 m/s), and CALPUFF overestimated the contribution of the highway. Given the equivalence

between the “emissions in” and the “emissions out” scenarios, the remaining discussion on source contributions considers the “emissions out” simulations only.

4.4.1 Carbon Monoxide

Total CO emissions in the study area is913g/s (EEAmax), with highway emissions accounting for 19% (170 g/s) and point sources for 81% (743 g/s). The point sources CN and Holcim1&2 account for almost all emissions in the latter category (95%). However, the spatial distribution of the sources, their variable geometry (point, area, etc.) and thus different dispersion characteristics prohibits any direct correlation between emissions magnitude and the contribution at a receptor. In particular, Highway emissions are extended over a large area 17000m × 18m, while point sources are more spatially confined. Figure 18 shows the contribution of point sources and Highway emissions to the CO concentration at Enfeh, both on a daily and weekly basis. CALPUFF under-predicted the observed 24-hour average concentration during the 1st week (factor of 3), thus promoting the likelihood of underestimation of point source emissions, given that these were major contributors during this period (65-80%) (Figure 18-a), particularly CN, which is the closest to Enfeh. However, CALPUFF predictions matched well with the daily average concentration during the 2nd week, where highway emissions dominated the contribution to the CO concentration (95%), indicating less uncertainty in estimating highway emissions. Figure 18-b shows the contribution of both source categories to the highest weekly average concentration, where highway emissions contribute to around 47% of the

predicted average, depicting the significance of emissions from this source category in the study area.

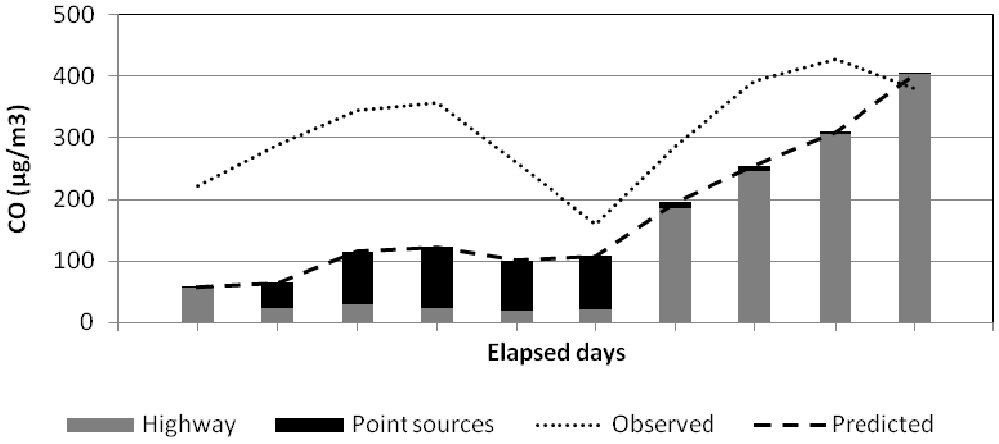

a- Time series of the 24-hour average concentration (Jan01-Jan11)

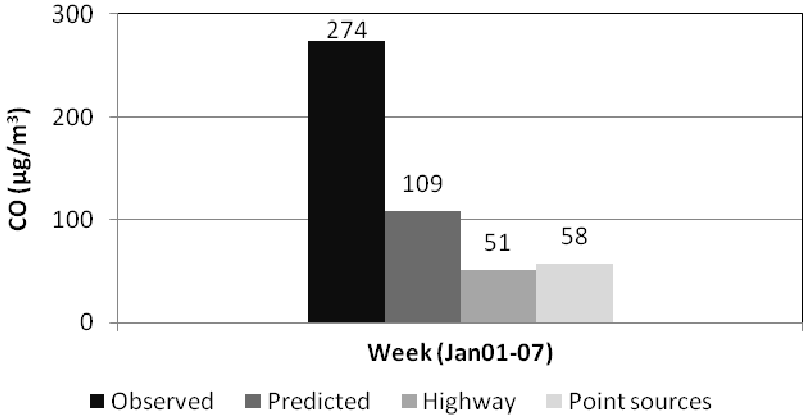

b- Highest 1-week average

Figure 18. Source contribution to CO concentration at Enfeh

At Chekka (see Figure 19), highway emissions accounted for almost all the CO concentration for both daily and weekly averaging times, except for the period Jan28-30, when point sources contributed to around 40-60% of the 24-hour average concentration.

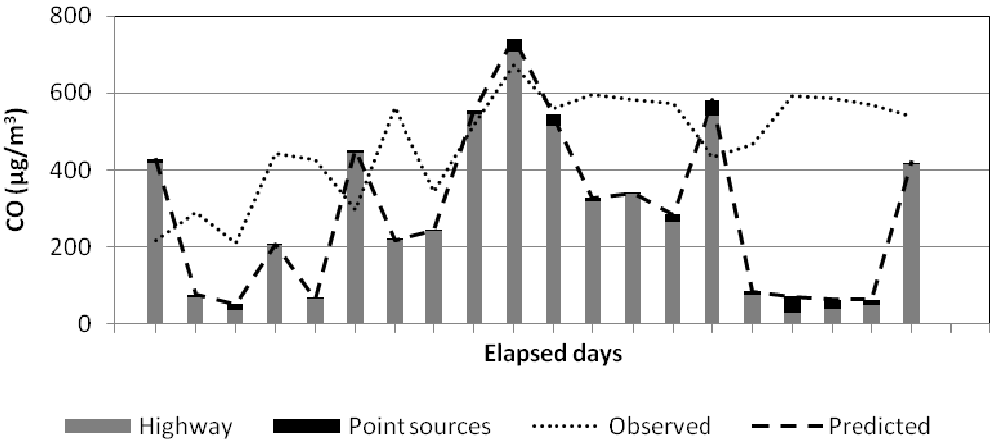

a- Time series of the 24-hour average concentration (Jan12-Feb02)

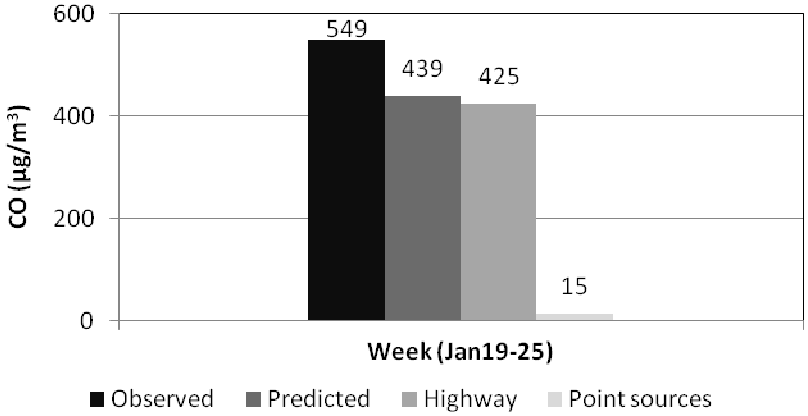

b- Highest 1-week average

Figure 19. Source contribution to CO concentration at Chekka

During this period however (Jan28-30), CALPUFF exhibited a noticeable under-prediction of observations, as opposed to the very good agreement during other days (Figure 19-a), when highway emissions contributed to more than 96% of the predicted

concentrations. Again, under-predictions of observed concentrations may be attributed to underestimations of point sources emissions.

As indicated earlier, CALPUFF underestimated the maximum 24-hour average CO concentration at Fih. Figure 20 further depicts this underestimation over the simulation period (June15-July05). Point sources accounted for around 85% of the predicted concentration during some days (June25-26) (Figure 20-a), and for 55% of the highest weekly-average (Figure 20-b). On the other hand, higher predicted concentrations, (relatively closer to observations) are noticed when highway emissions dominate the contribution to CO levels, namely the 2nd half of the simulated period, when contribution of highway emissions ranged between 45-70%. This further promotes the likelihood of underestimations of CO emissions from point sources, or the presence of significant boundary CO concentration contributed by domestic sources (unaccounted for in CALPUFF simulations).

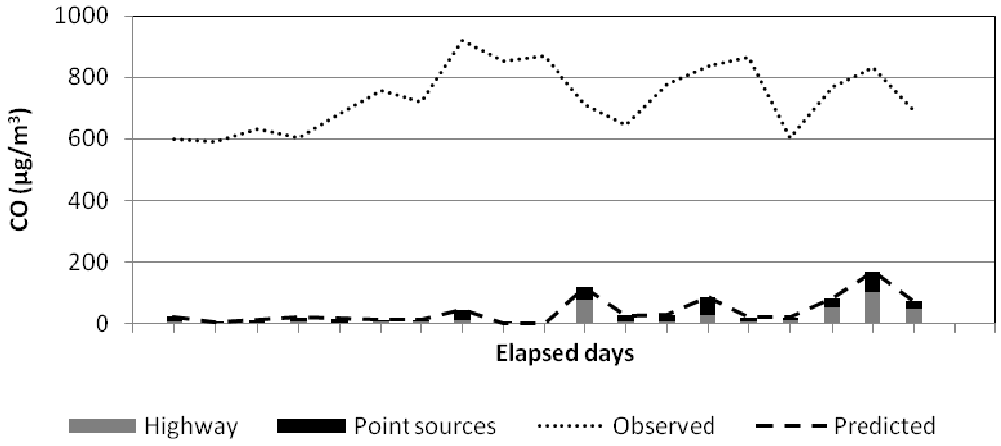

a- Time series of the 24-hour average concentration (June15-Jul05)

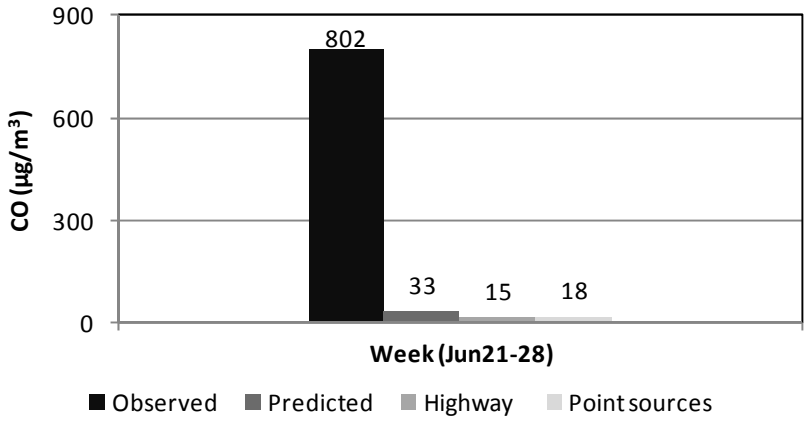

b- Highest 1-week average

Figure 20. Source contribution to CO concentration at Fih

Kfarhazir reveals a similar trend (Figure 21), with under-predictions of the 24-hour average concentration when point sources dominate the contribution, namely the 1st week of the simulation period (Figure 21-a). However, highway emissions dominated the contribution to CO levels at this receptor, reaching up to 95% at some days, and where CALPUFF predictions matched well with the magnitude and temporal pattern of observations (less than a factor of two under-prediction). Furthermore, highway emissions contributed to 77% of the highest weekly average concentration at Kfarhazir (Figure 21-b).

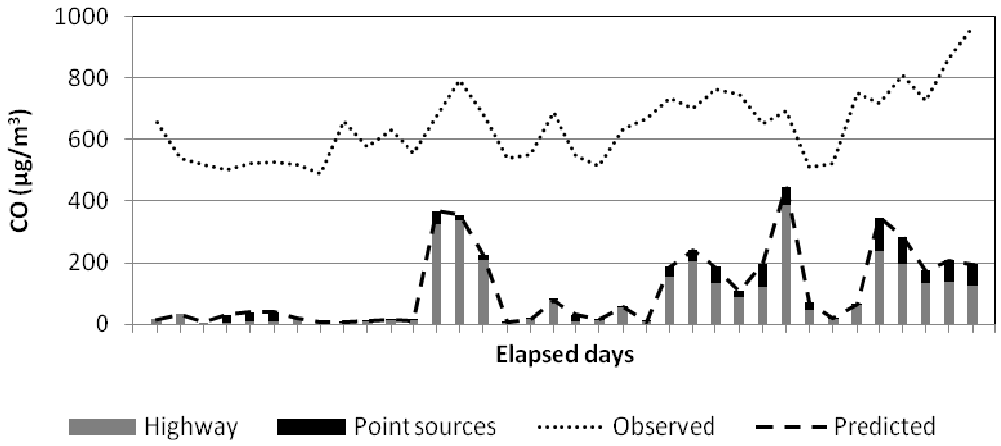

a- Time series of the 24-hour average concentration (July06-Aug10)

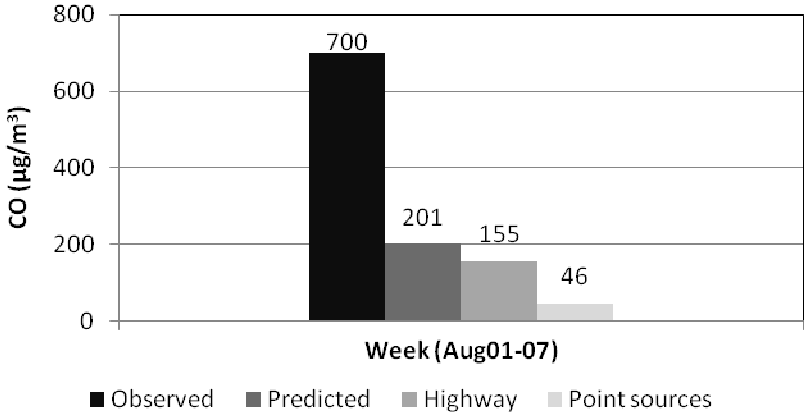

b- Highest 1-week average

Figure 21. Source contribution to CO concentration at Kfarhazir

At Kifraya, highway emissions contributed 100% of the predicted concentration for all days, with over-predictions of the observed concentration, and thus was excluded from the analysis. Overall, while the CO emission rate (EEA_{max}) represents total emissions in the study area, frequent under-predictions are noticeable, particularly at Fih and Kfarhazir, which can be attributed to underestimation of CO emissions from point sources. Also,

vehicular emissions are significant contributors to the CO concentration in the study area, with this contribution decreasing at farther locations. To provide a contribution assessment over the entire area, Figure 22 shows contour lines delineating CO levels contributed by highway and point sources emissions separately, during two months of the year.

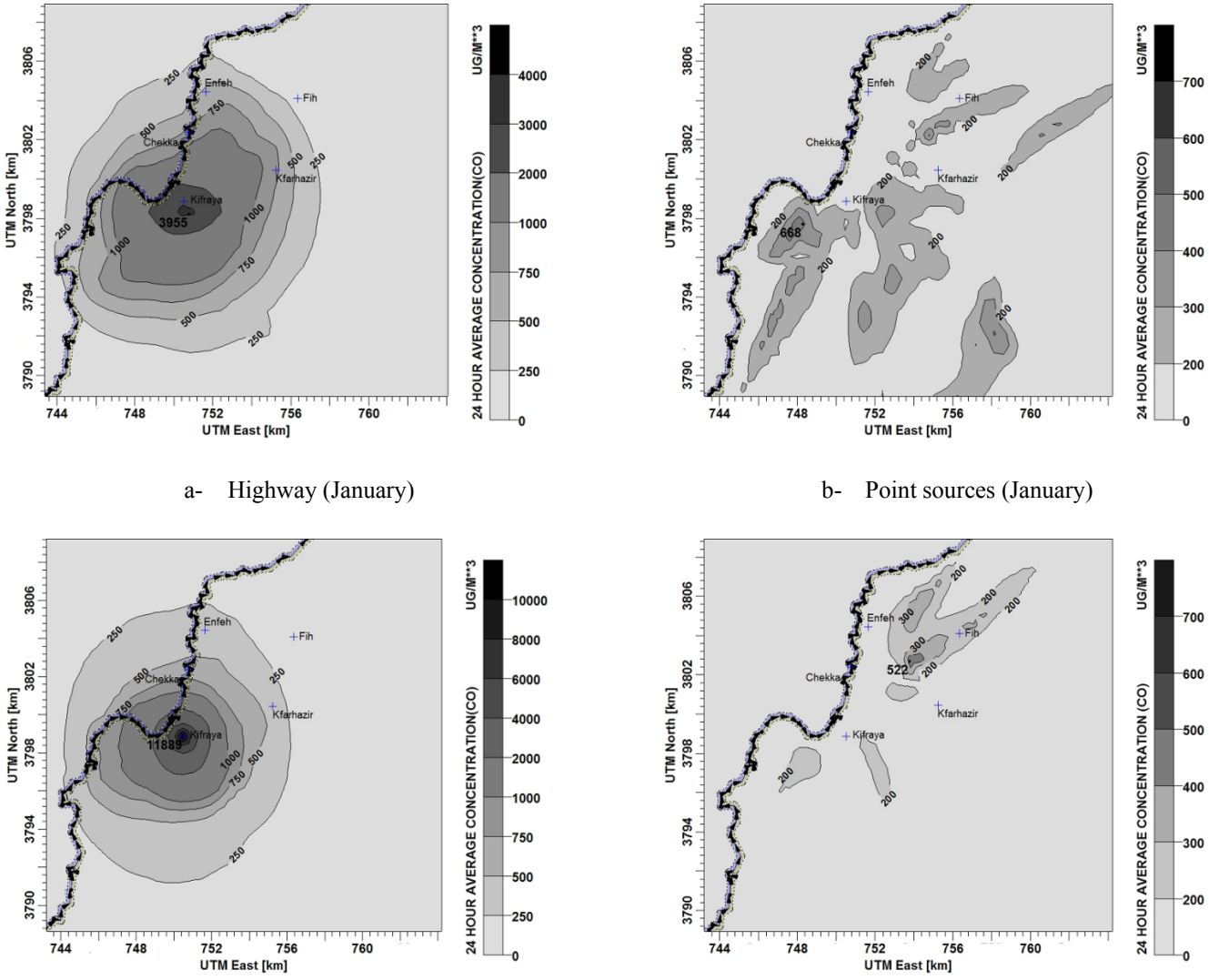

a- Highway (January)

b- Point sources (January)

c- Highway (June/July)

d- Point sources (June/July)

Figure 22. Spatial distribution of the 24-hour average CO concentration(µg/m^3) during winter and summer

The highest 24-hour average CO concentration contributed by highway emissions increased by around a factor of three during summer (3955 µg/m3 during January vs. 11889 µg/m3 during July), but occurred at the same location, close to Kifraya. Also, summer times are characterized by higher near-source accumulations (Figure 22-c), primarily due to the frequent occurrence of stagnation hours. For instance, Enfeh and Kfarhazir(relatively distant receptors from highway emissions) witnessed CO levels of 500 and 750 µg/m3 during winter (Figure 22-a), respectively, as opposed to lower levels (250 µg/m3) during summer. Highway emissions are thus transported to farther locations during winter times, but always with concentrations lower than the USEPA standard. On the other hand, the peak 24-hour average CO concentration contributed by point sources decreased from 668 µg/m3 during winter to 522 µg/m3 during summer (Figure 22 b-d). Furthermore, winter times were characterized by larger areas affected by higher CO levels, particularly southern regions, albeit lower than the standard.

4.4.2 Nitrogen Dioxide (NO_2)

Total NO_x emissions in the study area reached 1267g/s, with highway emissions accounting for 63% (800g/s) and point sources for 37% (467g/s). In previous sections, CALPUFF was shown to generally under-predict the measured NO_2 concentration in the study area for all averaging times. Despite of this, predicted concentrations exceeded the NO_2 1-hour average standard. The contribution of the two categories to NO_2 concentration at different receptors is shown in Figure 23 (a-d). The predicted 24-hour average concentration matched well observations at Chekka, except for two days (Jan16-17), when

considerable under-prediction is evident (Figure 23-a). Highway emissions accounted for 95% of the NO_2 concentration at this receptor for all days.

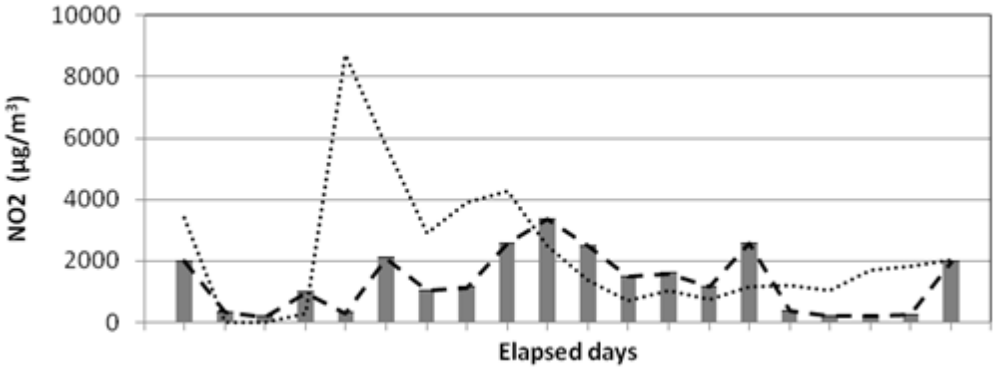

a- Chekka (Jan12-Feb02)

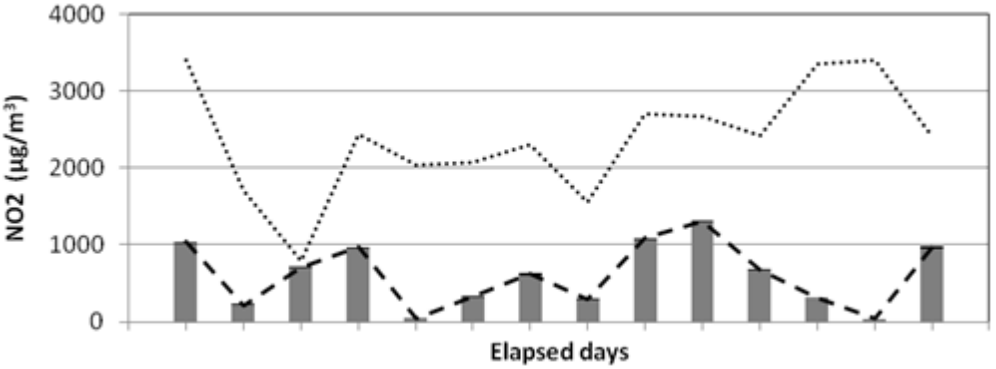

b- Kfarhazir (Mar02-15)

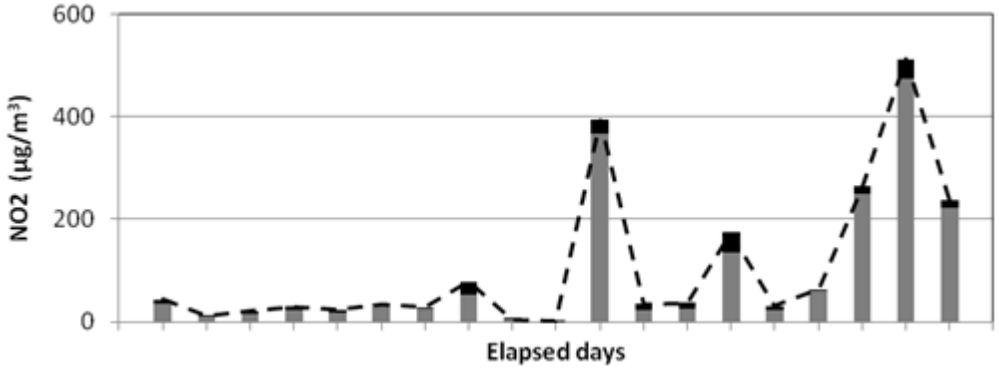

c- Fih (June15-Jul05)

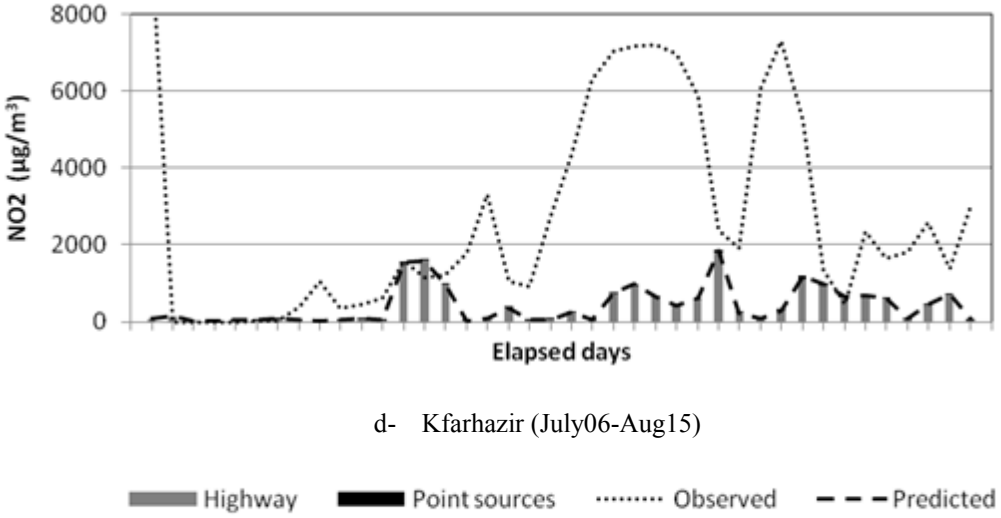

d- Kfarhazir (July06-Aug15)

Figure 23. Source contribution to the 24-hour average NO_2 concentration at several receptors

At Kfarhazir (March02-15)(Figure 23-b), CALPUFF under-predicted the observed concentration (a factor of three), but was able to reproduce the temporal trend over the time period. Highway contribution prevailed also at this receptor, with a percentage of >95%. At Fih, point sources contributed up to 36% during some days (Figure 23-c), but with significant under-predictions of observations (two to three orders of magnitude), which are hence not shown. While this could be attributed to under-estimation of point sources emissions, there remains the possibility that other potential sources unaccounted for in the simulations, are contributing to such elevated concentrations. Furthermore, CALPUFF generally captured the temporal fluctuation in the concentration distribution at this receptor (Fih), indicating that a higher emission rate would result in better matching of observed concentrations. During another period at Kfarhazir (Figure 23-d), the predicted concentration was a factor of five less than the observed, with highway emissions dominating the contribution (90%), except for July10-14, when point sources contributed

around 35%. Note that this period (July10-14) was associated with considerable under-predictions.

The spatial distribution of NO_2 levels contributed by the two categories is shown in Figure 24. Summer times were characterized by higher accumulation of NO_2 concentration for both highway and point sources. Peak concentrations contributed by point sources increased during summer and occurred at a different location (South-west in winter and North in summer) (Figure 24-b,d). Also, Larger areas were affected by point sources emissions during summer, with relatively higher concentrations. On the other hand, highway emissions contributed to larger areas during winter, indicating longer transport distances. The peak concentration occurred at the same location near Kifraya, and increased by slightly more than a factor of two in summer.

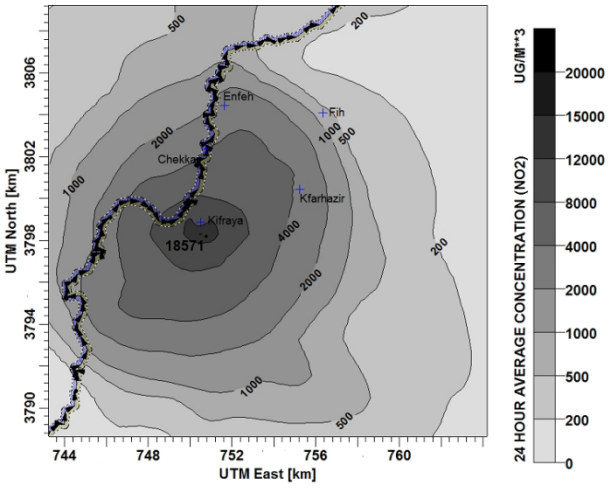

a- Highway (January)

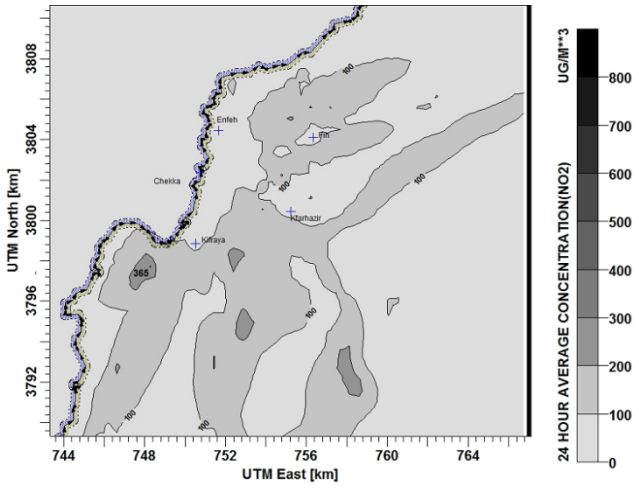

b- Point sources (January)

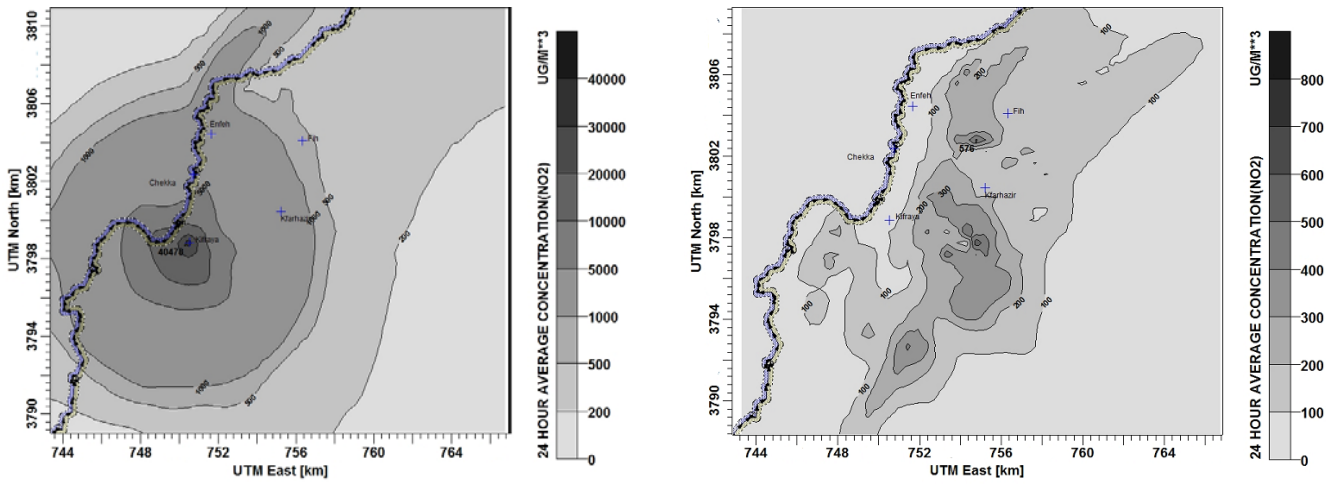

c- Highway (June/July) d- Point sources (June/July)

Figure 24. Spatial distribution of the 24-hour average NO_2 concentration($\mu g/m^3$) during winter and summer

4.4.3 Sulfur Dioxide (SO_2)

SO_2 emissions are limited to point sources, with a total of 1312 g/s, and thus was excluded from source apportionment analysis. The spatial distribution of SO_2 concentration contributed by point sources was presented earlier (Figures 15-b and 16-b).

4.4.4 Dust (PM_{10})

Sources contributing to PM_{10} emissions are area sources (quarrying sites) (197 g/s) and point sources (2773 g/s), accounting for 7 and 93% of total emissions (2784g/s), respectively. Measurements of ambient PM_{10} concentrations were limited to one or two days at a receptor, allowing for no generalizations on the contribution of these sources at specific receptors. Irrespective, the contribution of each source category to PM_{10} levels is examined in the context of spatial analysis of the concentration distribution. Furthermore, the analysis is limited to a single period of the year to reflect on the contribution magnitude

of each source category, rather than the spatial distribution (areas affected) which is expected to have similar patterns as that of NO_2 and SO_2. Figure 25 shows contour lines of PM_{10} levels in the study area contributed by point and area sources during summer times (July), which systematically revealed higher accumulation levels.

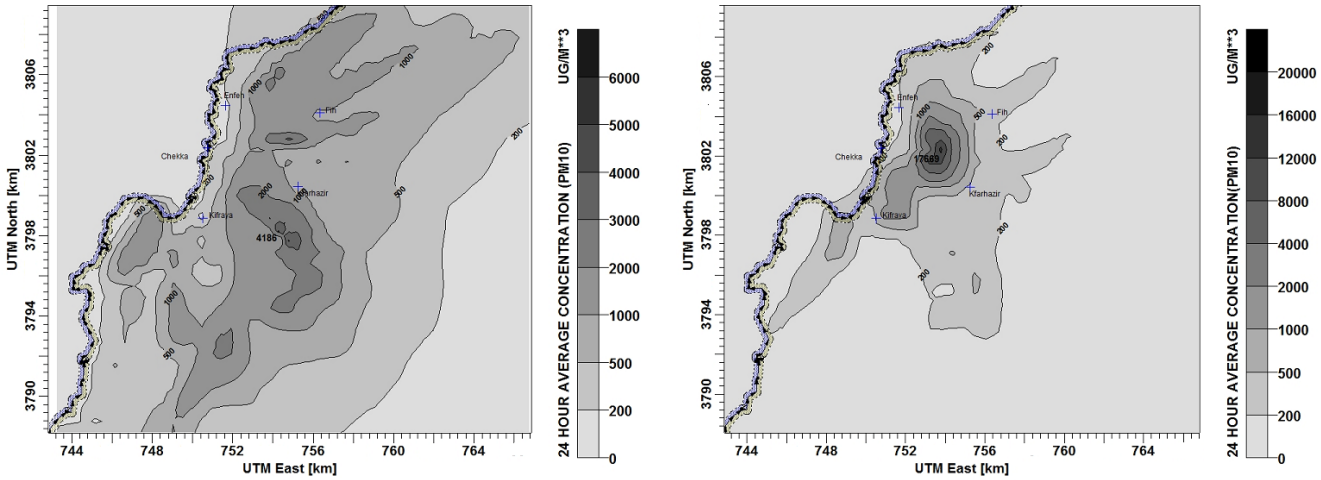

a- Point sources (July) b- Area sources (July)

Figure 25. Spatial distribution of the 24-hour average PM_{10} concentration($\mu g/m^3$) during summer

Emissions from point sources affected almost all the study area with concentrations exceeding the 24-hour average standard (150 $\mu g/m^3$), with inner areas witnessing higher PM_{10} levels than coastal ones (Figure 25-a). The peak 24-hour average concentration contributed by point sources reached 4186 $\mu g/m^3$ south to Kfarhazir. On the other hand, emissions associated with quarrying (area sources) affected a smaller part of the study area, albeit higher accumulation levels near the sources. The peak concentration reached about 17700 $\mu g/m^3$, and occurred close to the CN quarry, indicating weak dispersion and shorter transport.

4.4 Sensitivity Analysis

4.4.1 Coastal Fumigation

CALPUFF simulations without coastlines were conducted at different receptors and time periods to examine the significance of coastal fumigation in the study area under different terrain and meteorological settings. While the discussion is limited to CO, the results can be generalized to other pollutants, given that these are emitted simultaneously and with minimal chemical transformations, if any. Furthermore, CO emission rate was most representativeness of the study area, at which CALPUFF predictions matched well with field observations. Figure 26 shows 1-hour average time series of the predicted CO concentration in the two scenarios (i.e. with and without accounting for coastlines effect in simulations), with complete overlap at all receptors. The results indicate thus the equivalence of the two scenarios at all receptors and under different meteorological conditions (time periods), depicting that coastal fumigation is of little significance at the monitored locations. Note that this was the case for the other receptors (Enfeh and Kifraya) (not shown). As discussed earlier, highway emissions dominated the contribution to CO levels at the close receptors (Chekka, Enfeh and Kifraya). Thus, this analysis focused on Fih and Kfarhazir because plumes emitted from point sources contributed to CO levels at these receptors, and hence coastal fumigation, if any, would primarily affect the transport of these plumes and subsequently their contribution at these locations. Furthermore, coastal fumigation did not affect the spatial distribution of CO concentrations in the study area.

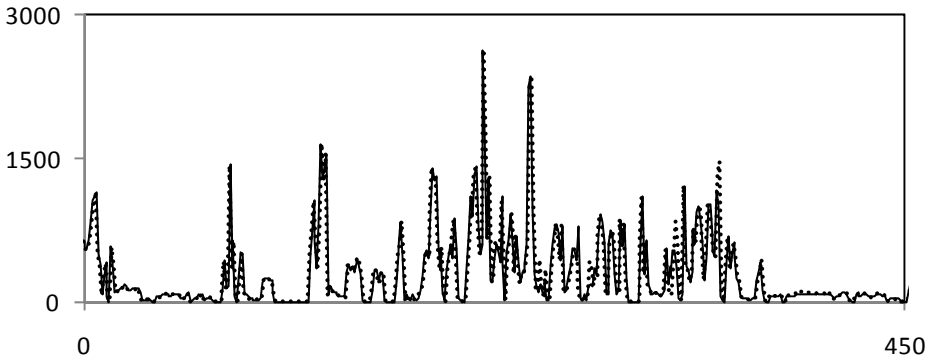

a- Chekka (Jan11-Feb02)

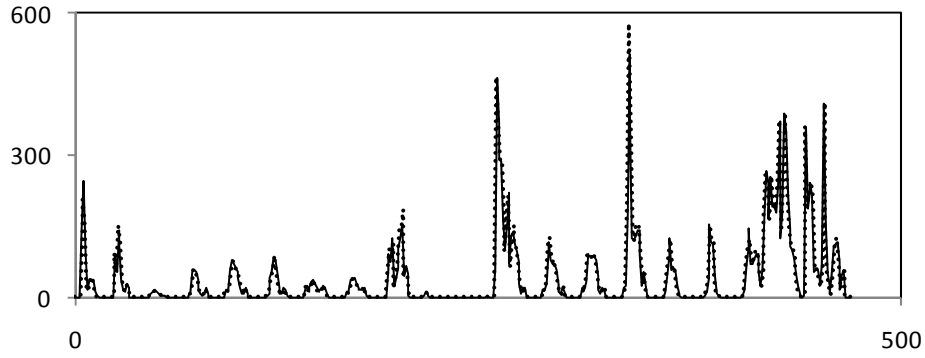

b- Fih (June15-July05)

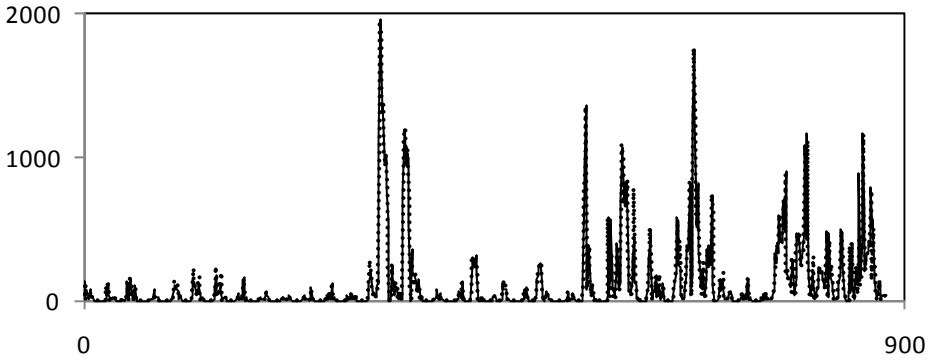

c- Kfarhazir (July05-Aug16)

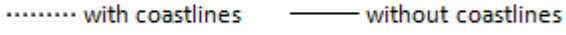

Figure 26. Time series (hourly) of CO (µg/m^3) with and without coastlines

4.4.2 Chemical Transformations

Uncertainty in the obtained results is also discussed in the context of sensitivity analysis of CALPUFF's output to chemical transformations of NO_x to nitrate aerosols, and SO_2 to sulfates (SO_4). The MESOPUFF II scheme within CALPUFF utilizes first-order reaction kinetics for these transformations, and computes daytime conversion rates for chemical reactions. The SO_2 to SO_4 conversion rate is proportional to the relative humidity, background ozone concentration, and inversely proportional to a stability index (ranging between 2-6 based on five PG stability classes). The NO_x conversion rate does not depend on the relative humidity, but is proportional to the ozone concentration, plume NO_x concentration, and inversely proportional to the stability index. As for nighttime conversion rates, model defaults of SO_2 conversion rate at 0.2%/hour, and NO_x rate at 2%/hour were used. To compare CALPUFF's predictions under the two scenarios (i.e. with and without simulating chemical transformations), Figure 27 shows time series of the 1-hour average NO_2 concentration predicted via the two scenarios at different receptors. While time series of both under-predicted observed NO_2 concentrations, particularly at Fih (several orders of magnitude and hence not shown), they coincided with each other, indicating little to no NO_x reactions. Only at Fih (Figure 27-c), predicted NO_2 concentrations slightly decreased when chemical transformations (CT) were simulated, reflecting the significance of longer transport distances on inducing chemical reactions. Note that the statistical parameters calculated upon modeling chemical transformations, and the spatial distribution of the NO_2 concentration, exhibitedno significant differences compared to base-case simulations (data not shown). SO_2 exhibited similar results, with little significance to chemical transformations at all receptors.

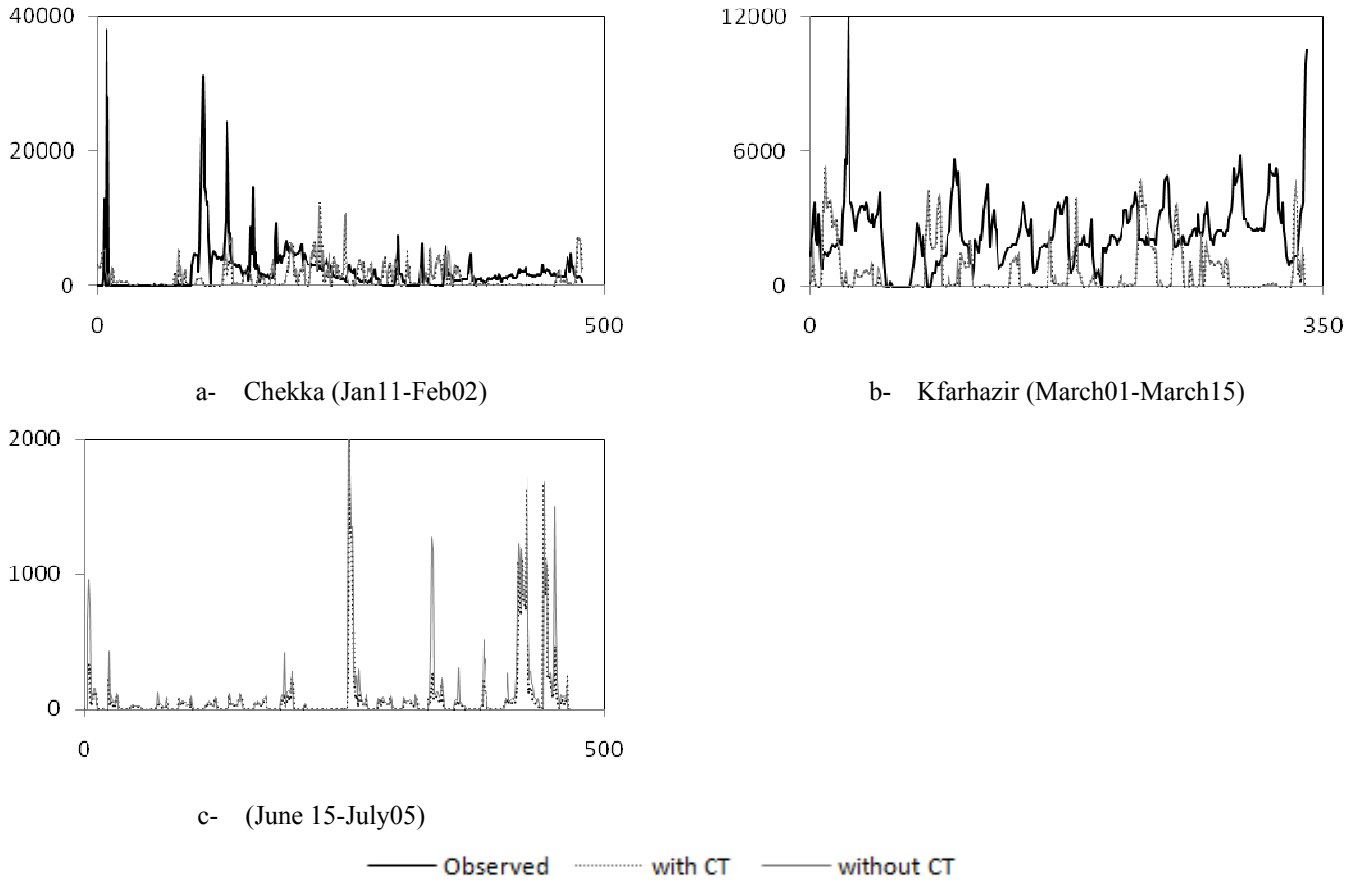

a- Chekka (Jan11-Feb02)

b- Kfarhazir (March01-March15)

c- (June 15-July05)

Figure 27. Time series (hourly) of the NO2 concentration (µg/m^3) with and without CT (Chemical transformations)

4.5 CALPUFF vs. ADMS4

Comparative assessments of the performance of dispersion models under equivalent settings is adequate in regulatory contexts, particularly when uncertainties characterize several components of the assessment. ADMS4 is a steady state Gaussian dispersion model, with advanced algorithms for the treatment of atmospheric turbulence characteristics and its spatial variability via the Planetary Boundary Layer (PBL) theory. One acknowledged limitation of ADMS4 is that treatment of regions of stagnation (calm hours) is beyond its capabilities. Similar to the base-case simulations conducted by

CALPUFF, simulations using the five emission rates were also conducted at all receptors and time periods using ADMS4. Note that the meteorological data used in ADMS4were limited to single station records of wind speed, wind direction, ambient temperature and relative humidity associated with field measurements of the concentration of criteria pollutants. For the discussion below, predictions of the two models (CALPUFF and ADMS4) are to be compared against observations using statistical analysis. Also, this comparison considers the CALPUFF-based estimations of the emission rates, namely EEA_{max} as the emission rate for CO and SO_2, and EPA_{max} for NO_x and PM_{10}. Due to the large dataset, comparison is conducted for each pollutant at one receptor, namely those where ADMS4 showed best performance. For instance, ADMS4 showed best performance for NO_x at Chekka, PM_{10} at Fih, and SO_2 at Kifraya. As for CO, Enfeh was considered due to the difference in estimated emission rate by the two models. Table 21 summarizes the results of this comparative assessment, where at each receptor, data were aggregated for all run periods.

Table 21. Comparison of CALPUFF and ADMS4 performance at selected receptors for the criteria pollutants

	CALPUFF				ADMS4			
Statistical parameter / Pollutant	FB	MG	NMSE	FAC2(%)	FB	MG	NMSE	FAC2(%)
CO (Enfeh)	-0.04	1.2	4	24	0.26	1.65	3.7	24
NO_x (Chekka)	0.67	3.1	4	22	0.03	0.94	6.3	27
SO_2 (Kifraya)	1.5	4.3	22	35	0.06	2.34	4.1	46
PM_{10} (Fih)	-0.1	4.4	2.3	22	0.11	2.96	1.37	37

Both models generally revealed acceptable performance at the specified receptors. At Enfeh, CALPUFF matched better with the mean CO concentration, while ADMS4 slightly under-predicted this mean. Both models showed comparable performance for the

other statistical parameters, with predictions within a factor of two of observations for 24% of the times. ADMS4 performed comparably to CALPUFF in predicting the NO_x, SO_2 and PM_{10}concentration at Chekka, Kifraya and Fih respectively, with CALPUFF generally under-predicting the mean. Note that ADMS4 simulation results were screened to remove those unreliable predictions associated with clam hours, which constituted a considerable percentage of all simulation periods. Furthermore, the above comparison was based on aggregated data for several simulation periods at each receptor, which does not reflect on performance under different meteorological conditions, and thus such results could not be generalized.

4.6 Emissions Reduction Assessment

This section examines the impact of compliance of point sources with the Emission Limit Values (ELV) set by the national Ministry of Environment (MoE) and international institutions. Except for CO, which consistently was at levels lower than the 1-hour average standard (40,000 $\mu g/m^3$), the spatial distribution of NO_2, PM_{10} and SO_2 concentrations in the study area is examined upon compliance of point sources. The ELV set by the MoE is an emission concentration of 500 mg/m^3, for pollutants with a mass flow of >10kg/hr (MoE 1996; MoE 2000), which is the case for all pollutants in the study area. Emission rates in compliance with these regulations were thus calculated as the product of these ELVs and the emissions flow rate, which is in turn dependent on the stack's inner diameter and flow exit velocity. Furthermore, the assessment is based on summer times, where frequently higher peak concentrations were noticed. Figure 28 shows contour plots of NO_2, PM_{10} and

SO_2 concentrations when all source categories were considered to be emitting, but with point sources complying with the ELVs.

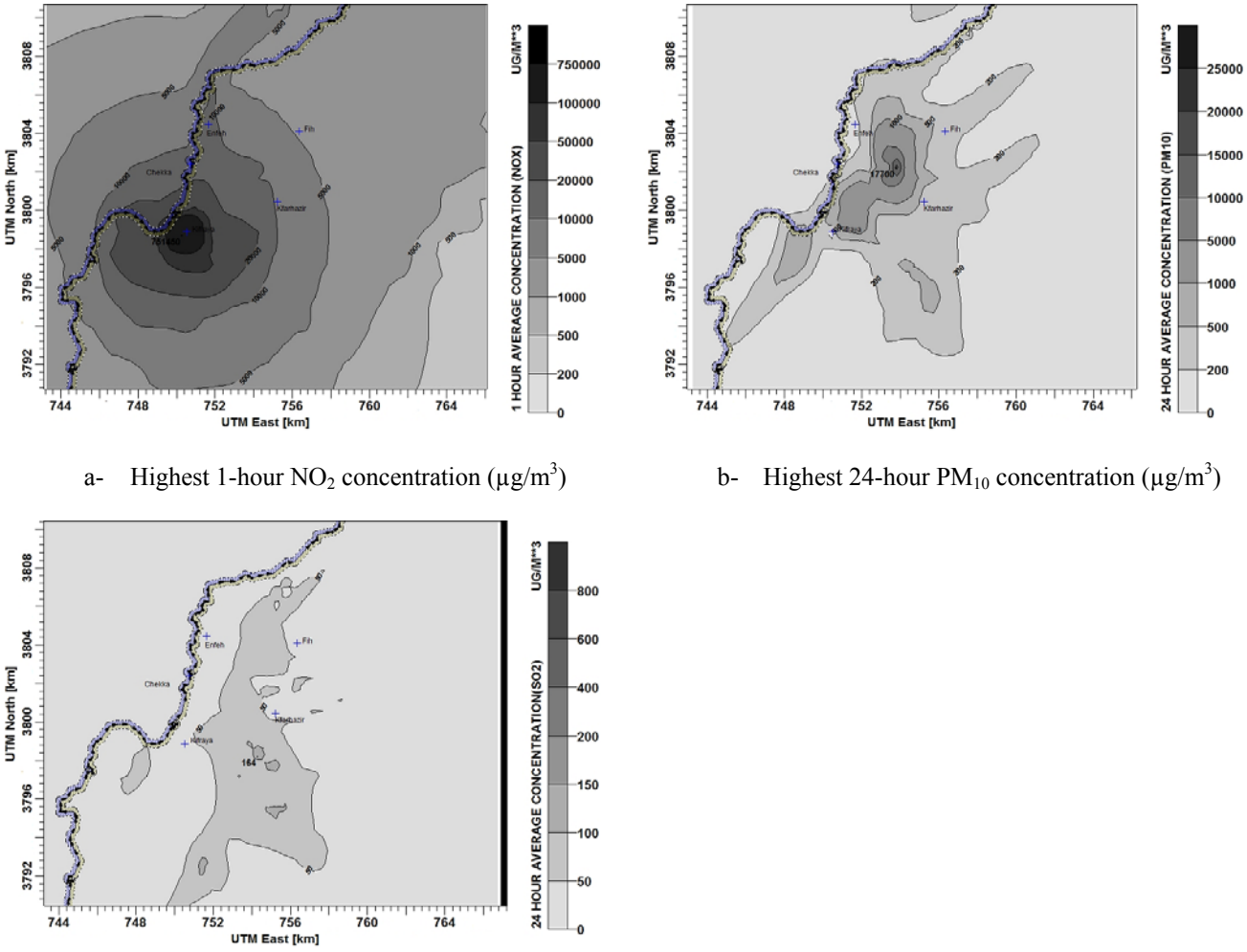

a- Highest 1-hour NO_2 concentration ($\mu g/m^3$)

b- Highest 24-hour PM_{10} concentration ($\mu g/m^3$)

c- Highest 24-hour SO_2 concentration ($\mu g/m^3$)

Figure 28. Spatial distribution of NO2, PM10 and SO2 levels with point sources complying with ELV

For NO_2, and as compared to the base-case scenario, no significant changes in the total area affected by standard-exceeding levels could be distinguished, mainly due to the prevalence of highway contribution on NO_2 concentrations. However, PM_{10} and SO_2 distribution revealed significant decreases in both the total area exceeding the standards

and the peak levels. The maximum 24-hour average PM_{10} concentration decreased slightly from 21,000 μg/m^3 (Figure 15-d) to 17700 μg/m^3, which is mainly contributed by quarrying sites. However, a decrease of 40-50% of the total area exceeding the 24-hour PM_{10} standard (150μg/m3) could be distinguished (Figure 28-b). As for SO_2, almost all the study area appears to be at levels lower than the 24-hour standard (196 μg/m^3) upon compliance (Figure 28-c), mainly due to the fact that only point sources contribute to SO_2 emissions. The maximum concentration decreased from 1673 μg/m^3(Figure 15-c) to 164 μg/m^3.

CHAPTER 5

CONCLUSION AND RECOMMENDATIONS

The MM5/CALMET/CALPUFF modeling system was used to simulate the dispersion of criteria pollutants emitted from various sources in and around an industrial complex in Chekka, North Lebanon. CALPUFF was used in a predictive emissions scheme, and the considered sources were assessed to be emitting at the conservative emission rates EEA_{max} for CO and SO_2 and EPA_{max} for NO_x and PM_{10}. CALPUFF performed well in matching field measurements at most receptors and simulated periods, and was able to capture temporal fluctuations in the concentration distribution. However, CALPUFF over-predicted observations at receptors very close to the sources, particularly highway emissions. The ambient concentration of criteria pollutants exceeded the standards over most of the study area, except for CO. Furthermore, CALPUFF was tested for its linear response to changes in precursor emissions via an emission sensitivity simulation set, and proved to be adding the contribution of each source at a receptor. Source apportionment revealed significant contributions of highway emissions to elevated levels of CO and NO_2, with point sources impacting distant areas, particularly during summer times. The Sensitivity analysis of CALPUFF output to coastal fumigation and chemical transformations appeared to be negligible. Comparative assessment of CALPUFF and ADMS4 was based on aggregate data analysis at each receptor due to limitations of the performance of ADMS4 during calm conditions, and revealed comparable performance of

the two models. Compliance of the various facilities with the ELVs improved the air quality within the modeling domain, except for NO_2.

Finally, meteorological and emissions uncertainties continue to limit adequate model validation and subsequently the credibility of air quality impact assessments. While spatially and temporally sufficient meteorological measurements are costly to obtain and often sparse to adequately characterize regional scale ambient state, prognostic numerical weather predictions, which are used in this study (mesoscale model MM5), are still questionable and resource-demanding. The "Hybrid" approach that employs coupling of meteorological simulations with observations to assimilate and construct the wind field are often recommended in similar cases, particularly where terrain complexity and spatially-variable land-sea flow patterns dominate the ambient meteorology. Also, short-term measurements and characterization of emissions from various sources would contribute to better evaluation of model performance and subsequently the reliability of an integrated assessment. In particular, while this study assumed temporally-uniform emissions, better characterization of the variability of source strengths is recommended, especially highway emissions which are subject to significant diurnal changes. To this end, representative siting of monitoring stations need to be discussed in the context of prevailing meteorology and simultaneous measurements at several collinear downwind receptors in order to examine model performance over the study area during a given time period.

REFERENCES

Anthes RA, Kuo Y-H, Hsie E-Y, Low-Nam S, Bettge TW. (1989). Estimation of skill and Uncertainty in regional numerical models. Quart J Royal.*Meteor Soc* 115:763-806.

ASTM (2000) Standard guide for statistical evaluation of atmospheric dispersion model performance. American Society of testing and materials, Designation D 6589-00. ASTM, 100 Barr Harbor drive, West Conshohocken, PA 19428-2959.

Barna, G., Schichtel, A. &Gebhart, K. A. (2006). Modeling regional sulfate during the BRAVO study: Part 2. Emission sensitivity simulations and source apportionment. *Atmospheric Environment, 40* (14), 2423-2435.

Banerjee, T. (2010). Assessment and model performance evaluation of air quality at Integrated Industrial Estate-Pantnagar. Doctor of Philosophy Thesis, Department of Environmental Science, G.B. Pant University of Agriculture and Technology, Pantnagar, India.

Beck, MB., Ravetz, JR., MulkeyLA, Barnwell TO. (1997). On the problem of model validation for predictive exposure assessments. *Stoch Hydrol Hydraulics* 11: 229-254

Chang, J.C., Hanna, S.R. 2004. Air quality performance evaluation. *Meteorology and Atmospheric Physics* 87: 167-196.

Cheung, H.-C., Wang, T., Baumann, K., Guo, H., 2005. Influence of regional pollution outflow on the concentrations of fine particulate matter andvisibility in the coastal area of southern China. *Atmospheric Environment* 39, 6463-6474.

Colvile, R. N., Woodfield, N. K. &Carruthers, D. J. (2002). Uncertainty in dispersion modeling and urban air quality mapping. *Environment Science and Policy, 5* 207-220.

Denby, B., Laupsa, H. &Larrson, S. (2009). Source apportionment of particulate matter (PM2.5) in an urban area using dispersion, receptor and inverse modelling. *Atmospheric Environment, 43* 4733-4744.

EEA. (2009). EMEP (Cooperative programme for monitoring and evaluation of the long-range transmission of air pollutants in Europe) / EEA (European Environment Agency) air pollutant emission inventory guidebook 2009, Technical guidance to prepare national emission inventories. EEA Technical Report No 9/2009, Copenhagen, Denmark.

El-Fadel, M. and Abi-Esber, L. (2011). Simulating industrial emissions using ADMS4: Model performance and source emission factors. *Journal of the Air & Waste Management Association* (tentatively accepted – second revision).

El-Fadel, M., Abi-Esber, L., Ayash, T. (2009). Managing emissions from highly industrialized areas: Regulatory compliance under uncertainty. *Atmospheric Environment* 43: 5015-5026.

El-Fadel, M., Zeinati, M., Ghaddar, N., Mezher, T. (2001). Uncertainty in estimating and mitigating industrial related GHG emissions. *Energy Policy* 29: 1031-1043.

EPA. (2009). *Air dispersion modeling from industrial installations guidance note (AG4).* Draft for public consultation, Environmental Protection Agency, Office of Environmental Enforcement, Johnstown Castle Estate, Wexford, Ireland.

Fox DG., (1984). Uncertainty in air quality modeling. B *Amer-Meteor Soc* 65: 27-36.

Fushimi, A., Kawashima, H. &Kajihara, H. (2005). Source apportionment based on an atmospheric dispersion model and multiple linear regression analysis. *Atmospheric Environment, 39* (7), 1323-1334.

Gifford Jr., F.A., (1976). Consequences of effluent releases.*Nuclear Safety* 17 (1), 68–86.

Holmes, N.S., Morawska, L. (2006). A review of dispersion modeling and its application to the dispersion of particles: An overview of different dispersion models available. *Atmospheric Environment* 40: 5902-5928.

http://www.epa.gov/air/criteria.html

Hueglin, C., Devos, W., Gehrig, R., Hofer, P., Kobler, J., Stahel, W.A., Wolbers, M., Baltensperger, U., Monn, C. (2000). Source apportionment of PM10 in Switzerland by application of a multivariate receptor model. Journal of Aerosol Science 31, 891–892.

Karam and M. Tabbara, (2004). Air Quality Management and Estimated Health Impact of Pollutants in Urban and Industrial Areas, Chekka and Koura Region, Lebanese American University, United States Agency for International Development USAID Grant No. 268-G-00-02-00223-00.

Kobrossi R, Nuwayhid I, El-fadel M; Sibai A and Khogali M (2002). Respiratory health effects of industrial air pollution in children, *International journal of environmental health research.*

Levy, J., Spendler, J. D. &Hlinka, D. (2002). Using CALPUFF to evaluate the impacts of power plant emissions in Illinois: model sensitivity and implications. *Atmospheric Environment, 36* (6), 1036-1075.

Longhurst, J. W., Beattie, C. I. &Woodfield, N. K. (2001). Air quality management: evolution of policy and practice in the UK as exemplified by the experience of English local government. *Atmospheric Environment, 35* (8), 1479-1490.

Macintosh, D., Stewart, J. & Myatt, T. (2010). Use of CALPUFF for exposure assessment in a near-field, complex terrain setting . *Atmospheric Environment, 44* (2), 262-270.

Mirasgedis, S., Hontou, V., Georgopoulo, E., Sarafidis, N.,Gakis, D.P. Lala., A. Loukatos, N. Gargoulas, A. Mentzis, D. Economidis, T. Triantafilopoulos, K. KoriziG.,Mavrotas, N.(2008). Environmental damage costs from airborne pollution of industrial activities in the greater Athens, Greece area and the resulting benefits from the introduction of BAT activities, *Environmental Impact Assessment Review* 28: 39–56

MoE (Ministry of Environment) (2000).National Standards for Environmental Quality. Prepared in the Context of the Strengthening the Permitting and Auditing System for Industries (SPASI), MoE, Beirut, Lebanon

Pasquill, F. (1961). The estimation of the dispersion of windbornematerial. *Meteorology Magazine* 90 (1063), 33–40.

Rama Krishna, T. V., Reddy, M. K. & Reddy, R. C. (2005). Impact of an industrial complex on the ambient air quality: Case study using a dispersion model. *Atmospheric Environment, 39* (29), 5395-5407.

Sokhi, R., Fisher, B., et al. (1998). Modelling of air quality aroundroads. In: Proceedings of the 5th International Conference onHarmonisation with Atmospheric Dispersion Modelling forRegulatory Purposes, Greece.

USEPA (United States Environmental Protection Agency) (1994). *Compilation of air pollutant emission factors, AP-42,* Fifth Edition. Office of Air Quality Planning and Standards, Emission Inventory Branch.

USEPA (United States Environmental Protection Agency) (1999) PCRAMMET User's Guide, Office of Air Quality Planning and Standards, Emissions, Monitoring and Analysis Division, USEPA (United States Environmental Protection Agency), Research Triangle Park, North Carolina (1999).

WHO (World Health Organization) (2005) WHO Air Quality Guidelines Global Update 2005 Report on a working group meeting, WHO (World Health Organization), Bonn, Germany: 18–20 October 2005.

Whyatt, J.D. Whyatt, S.E. Metcalfe, J. Nicholson, R.G. Derwent, T. Page and J.R. Stedman. (2007). Regional scale modeling of particulate matter in the UK, source attribution and an assessment of uncertainties, *Atmospheric Environment* 41, 3315–3327.

World Bank-UNIDA (United Nations Industrial Development Agency)-MoE (Ministry of Environment). (1998). Industrial Pollution Control Lebanon First Draft. Prepared by TEBODIN Consultants and Engineers for the World Bank, UNIDO and MoE-Lebanon, World Bank-UNIDA (United Nations Industrial Development Agency)-MoE (Ministry of Environment)